Journal of Cleaner Production xxx (xxxx) 134753

Contents lists available at ScienceDirect

Journal of Cleaner Production

journal homepage: www.elsevier.com/locate/jclepro

A prediction model for CO_2 concentration and multi-objective optimization of CO_2 concentration and annual electricity consumption cost in residential buildings using ANN and GA

Mohammadreza Baghoolizadeh [a], Mohammad Rostamzadeh-Renani [b], Seyed Amir Hossein Hashemi Dehkordi [a], Reza Rostamzadeh-Renani [b], Davood Toghraie [c, *]

[a] Department of Mechanical Engineering, Shahrekord University, Shahrekord, 88186-34141, Iran
[b] Energy Department, Politecnico di Milano, Via Lambruschini 4, 20156, Milan, Italy
[c] Department of Mechanical Engineering, Khomeinishahr Branch, Islamic Azad University, Khomeinishahr, Iran

ARTICLE INFO

Handling Editor: Cecilia Maria Villas Bôas de Almeida

Keywords:
GMDH type of artificial neural network
Time series prediction
Jeplus
Jeplus + EA software
Indoor air quality (IAQ)
Cooling set point
Heating set point

ABSTRACT

Environmental pollutants in the air have long been a great threat to the health and life of human society and the volume of these pollutants is rapidly increasing. Human beings spend most of their time in closed environments which highlights the demand for appropriate indoor air quality. This favorable air quality makes sense when the concentration of pollutants such as CO_2 that have penetrated the building space is reduced. This paper aims to predict a model for CO_2 emissions and optimize it for 6 cities of the U.S with different climates. Firstly, using the time series of GMDH type of artificial neural network, the amount of these pollutants was predicted monthly and annually from 2020 to 2025. The results show that the amount of CO2 pollutants during this period increases by 1–3% and 1.25–1.8% on a monthly and annual basis, respectively. In this research, to solve this huge predicament in the residential sector, 5 design variables are considered, which are the thermostat set point temperature of the air conditioning system for cooling and heating, the clothing insulation level of the residents' clothes for winter and summer seasons, and the amount of clean air that is transferred from the outside to the inside of the building by the air conditioning system. The goal is to simultaneously minimize CO_2 emissions and annual electricity consumption costs of the building and improve the thermal comfort of building occupants. Therefore, design variables and objective functions in JEPLUS software are defined. Afterward, they are analyzed based on the building's energy performance using EnergyPlus software. The elicited data are then transferred to JEPLUS + EA software, where they are optimized by the NSGA-II algorithm, which finally discovers the most optimal states so that users can select any state that is in line with their goals.

1. Introduction

It can be said that optimization is necessary and needed for every engineering system and that is why researchers tried to optimize their systems with different inputs and outputs with different existing algorithms (Jia and Wang, 2021; Srinivasareddy et al., 2021; Agarkov et al., 2022; Chen et al., 2021; Said et al., 2022). The proper way of energy consumption is one of the cases that has long been tried in human societies to prevent excessive energy loss (Qi et al., 2022; Liu et al., 2021; Tu et al., 2022; Yan et al., 2020; Ahmadi et al., 2019). Owing to the rapid industrial and economic developments in modern societies, the role of energy becomes more undeniable (Bellos et al., 2016; Jermsittiparsert, 2021). With the rapid development of urban housing construction and unsuitable patterns for energy consumption, the loss of energy resources is felt more in the world. The volume of energy loss in different industrial, commercial and residential sectors is significant and it is more striking in countries with severe weather conditions. According to US Energy Information Administration reports, from 2012 to 2040 (U. EIA, 2016), the amount of energy consumed in residential and commercial buildings comprises 20.1% of total delivered energy. This ratio is predicted to annually increase by 1.5% on a global scale. Furthermore, more than one-third of the energy consumed in residential buildings is for heating and cooling. On the other hand, excessive energy consumption leads to an increment in the emissions of greenhouse gases such as carbon dioxide (Bahrami et al., 2022). IPCC reported that the volume of greenhouse gases has more than doubled in 40 years be-

* Corresponding author.
E-mail address: Toghraee@iaukhsh.ac.ir (D. Toghraie).

https://doi.org/10.1016/j.jclepro.2022.134753
Received 7 September 2022; Received in revised form 1 October 2022; Accepted 14 October 2022
0959-6526/© 20XX

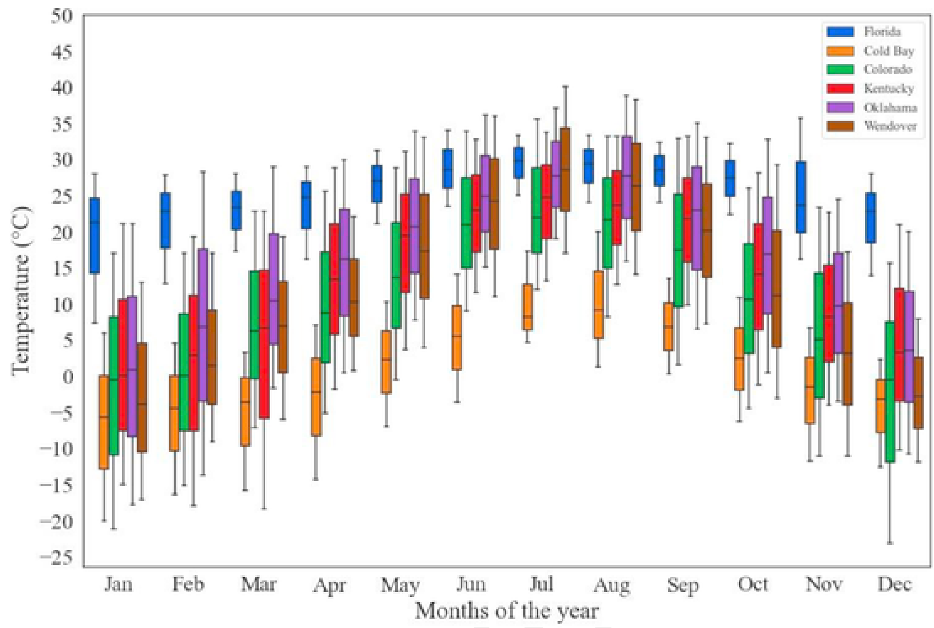

Fig. 1. Monthly temperature variations for all cities.

Table 1
Geographical specifications of selected cities.

State	City	Climate	Latitude (Degree)	Longitude (Degree)	Elevation (m)
Alaska	Cold Bay	Arctic climate	55.2	−162.72	23.8
Colorado	Niwot Ridge	H-Highland (alpine) climate	38.82	−104.72	1884
Florida	Key Biscayne	Aw-Tropical wet/ Dry season climate	24.56	−81.75	1.2
Utah	Wendover	Bsk-Semiarid steppe climate	40.72	−114.04	1292
Kentucky	Midway	Dfa-Humid continental (warm summer) climate	38.03	−84.6	301
Oklahoma	Rogers	Cfa-Humid subtropical climate	35.38	−97.6	398

tween 1970 and 2010, and it reached the value of 10 Gt CO2eq/yr at the end of this period (IPCC, 2014). Many researchers have stated that HVAC systems used for heating and cooling in buildings are the main ground for this issue (Khoukhi, 2018; Bakos, 2000; Chwieduk, 2003; Bojic et al., 2001). With the rise of energy consumption and subsequently burning of fossil fuel resources, irreparable damage is impelled to the environment, one of which is the increase in environmental pollutants. These pollutants have devastating effects on all sectors and jeopardize the health of human society (Sundell, 2004), and cause human death in some cases (Kumar et al., 2005). Because people spend a large part of their day indoors, the risk of having indoor pollutants increases (Byčenkienė et al., 2009; Dales et al., 2008; Leech et al., 2002). The aforementioned pollutants can penetrate indoor environments in various ways and endanger the health of residents. Scientists and researchers have conducted studies to address this issue which could help improve indoor air quality (IAQ) and reduce the effects of pollutants. Some researchers have based their studies on the use of plants that have air-purifying properties to help improve IAQ. Parhizkar et al. (2020) could reduce the amount of CO_2 concentration in an office building with some preparations. They could purify the air and reduce the concentration of CO_2 in the space by using a double-skin façade and placing 5 m^2 of Azolla algae per person. Jung et al. (Jung and Awad, 2021) also used Arka palm pots in the UAE university classroom and could ameliorate indoor air quality by up to 40%. Another group of researchers conducted their field studies in spaces with a larger number of inhabitants (schools, universities and office environments, etc.) to help people with their health by challenging themselves. Korsavi et al. (2020) worked on indoor air quality at a primary school in the UK and evaluated three factors affecting natural ventilation which are context (Santamouris et al., 2008; Gao et al., 2014; Heebøll et al., 2018), residents (Batterman et al., 2017) and building-related factors (Daniels and Bodkin, 2016) to achieve optimal air quality and concluded that for the CO_2 rate to be less than 1000PPM, each person should occupy space per 2.3 square meters. Haddad et al. (2021) experimentally worked on the air quality in the classroom of a school in Sydney, Australia which has subtropical climates. With the strategies they used in their research, they reduced the CO_2 concentration in the cold season from 2418 ppm to 1335. Jaber et al. (2017) could significantly decrease the amount of CO_2 concentration by changing the temperature of the thermostat in a school in Saudi Arabia. By changing the cooling temperature from 25 to 23 and from 23 to 20, they were able to reduce the CO_2 concentration from 1800 to 1000 PPM to 600PPM. Dorizas et al. (2015) worked on the role of ventilation rate and CO_2 concentration in student learning and found that there is a direct relationship between particle levels and CO_2 concentration on student health. Coley et al. (2007) also showed this effect more

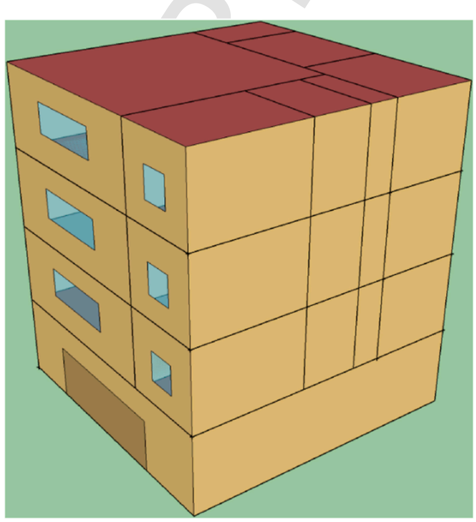

Fig. 2. The studied residential building.

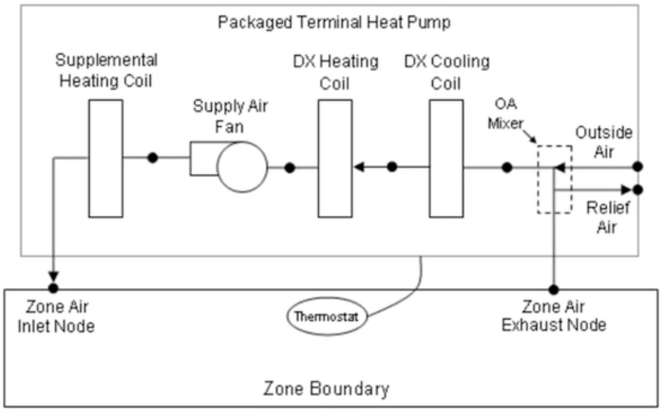

Fig. 3. General schematic of the Packaged Terminal Heat Pump system (US Department of Energy, 2014).

Table 2
Specifications of floor spaces of the studied building.

Zone	Floor area(m^2)
Bedroom 1	12
Bedroom 2	12
Kitchen	12
Hall	49
Bathroom1	6
Toilet	3
Staircase and Entrance	6
Parking	100

Table 3
Specifications of opaque construction materials.

constructions	Properties	Unit	Value
Interior wall	Total heat transfer coefficient (U)	$\frac{W}{m^2K}$	2.58
Exterior wall	Total heat transfer coefficient (U)	$\frac{W}{m^2K}$	0.7
Floor/ceiling	Total heat transfer coefficient (U)	$\frac{W}{m^2K}$	1.45
Door	Total heat transfer coefficient (U)	$\frac{W}{m^2K}$	3.5

prominently in another study. With the rising of CO_2 concentration, students 'concentration decreases and leads to students' headaches and fatigue (Australian Building Codes Board (ABCB) I.A.Q.H, 2018). Franco et al. (Franco and Leccese, 2020) discussed the correlation between the CO_2 concentration in indoor air and the number of people employed. Schibuola et al. (2016) investigated the effect of natural ventilation on indoor air quality and energy-saving. Amini et al. (2021) worked on indoor thermal comfort and indoor air quality and minimized them by using suitable glass glaze and shading. Another group of researchers conducted their studies on residential buildings. Belmonte et al. (2019) worked experimentally and simulated on 8 different apartments in Portugal. They calibrated their results on indoor air quality and estimated the root mean square error for simulated values between 5 and 10%. They also examined the impact of a mechanical ventilation system based on CO_2 demand. Pereira et al. (2017) conducted studies in residential buildings located in temperate climates and discovered that residents' behavior is effective in achieving IAQ levels and high thermal comfort, which is influenced by several factors concurrently. Canha et al. (2017) investigated the concentration levels of several chemical compounds (CO_2, CO, VOCs, formaldehyde, etc.) in a bedroom of a house in Portugal. They measured the concentration of the chemical compound for twelve consecutive days in August. Also, four different factors of ventilation regulation with window or door open or closed were analyzed. They also found that the air infiltration rate had a diluting effect on the concentration of internal pollutants. McGill et al. (2015) worked on eight different buildings in the UK which were built under the same insulation and airtight conditions. They inspected four houses with natural ventilation and four others with a mechanical ventilation system equipped with a heat recovery unit. They concluded that four mechanically ventilated houses could maintain CO_2 levels below 1000 ppm at any time in the living room and bedroom for both summer and winter periods. Noris et al. (2013) studied the effect of energy resilience on indoor environmental quality in sixteen apartments. They considered eight apartments with continuous mechanical ventilation and eight other apartments without mechanical ventilation. They reported results for a mixture of formaldehyde and nitrogen dioxide concentrations and found that apartments with continuous mechanical ventilation had a greater improvement in indoor quality than apartments without mechanical ventilation. Fan et al. (2021) investigated the CO_2 rate of sleeping people. They studied several men and women sleeping in the compartment and discovered that the average CO_2 rate for women was about 11 $\mp$ 1.4 L per hour, and for men, it was 8% higher than women. On the other hand, several researchers predicted CO_2 concentration and provided equations for it. The high cost of laboratory work as well as the large amount of time spent for producing and providing the sample coerces the researchers into focusing on numerical works and ultra-innovative algorithms and implementing various machine learning methods. Researchers need a series of experimental data to initiate numerical work and identify the factors influencing their aims. To design this data, a random sampling should be used to properly examine all the factors. There are several methods for random sampling, one of the best of which is the Latin Hypercube Sampling method (LHS) which was used by many researchers in various fields. An ideal choice must be made from random data. In most cases, choosing an ideal case is time-consuming and difficult, and as a result, it is better to use the help of machine learning and optimization algorithms. One of the useful approaches is the GMDH type of artificial neural network (ANN-GMDH), which can offer an accurate approximation of the model. The process of this network is to combine the input data in pairs to form neurons, each of which contains a polynomial. By placing the neurons next to each other, a layer is created, and in the same way, the neurons are combined in pairs to form the next layers until achieving a single neuron or output. The quality of the neural network is appropriate when the results predicted by the neural network are close to the simulation data. The neural network can be used to predict the goals of research (Band et al., 2020a, 2020b; Dianati Tilaki et al., 2020; Zhang et al., 2021; Shang et al., 2021; Lu et al., 2021; Said et al., 2021). This prediction can be done in line with time series prediction or a prediction model for data analysis. This type of neural network was used in various fields of mechanical engineering (Zhang et al., 2022; Nabipour et al., 2020). Shahsavar et al. (2019) investigated the effect of density and temperature of Fe_3O_4 nanoparticles on the viscosity and thermal conductivity of liquid paraffin-based nanofluids. Looney et al. (Loni et al., 2018) focused on the Petroleum/MWCNT nanofluid, a hemispherical cavity receiver that collects solar energy. They optimized the receiver by increasing the heat absorption and increasing the collector thermal performance by 13%. In recent years, many researchers have used this approach specifically in the fields of renewable energy, energy and building, etc. In previous studies, researchers focused more on reducing CO_2 concentrations indoors and did not consider the economic costs of the building. This issue appears when a natural or mechanical ventilation system is used to reduce the CO_2 concentration, and the air conditioning system should consume higher level of electricity to provide thermal comfort to the residents (Lin et al., 2022; Xie and Sun, 2022; Wang et al., 2022). However, the desired air quality and economic costs can be reached in the case of using appropriate design variables. In this paper, the amount of CO_2 is also predicted for the next few years so that researchers can use this data to expand their studies. Using the GMDH artificial neural network time series, the level of CO_2 pollutants was predicted on a monthly and annually basis from 2020 to

Table 4
Optical specifications of window glass.

Constructions	Properties	Unit	Value
Double-glazed windows	Total heat transfer coefficient (U(	$\frac{W}{m^2K}$	2.58
	Solar heat gain coefficient	–	0.703
	Visible transmittance	–	0.781

Table 5
Properties of the HVAC system.

Design parameter	Value
Cooling set point	25 °C
Cooling airflow rate	Auto size
Zone Cooling sizing factor	1.15
Cooling Coil Gross Rated Cop	3
Cooling coil	Single speed DX
Heating set point	22 °C
Heating airflow rate	Auto size
Zone heating sizing factor	1.15
Heating Coil Gross Rated Cop	2.75
Heating coil	Single-speed DX heat pump
No-load airflow rate	0
Outdoor airflow rate	Per person 0.009 m^3/s

Table 6
The values of electricity consumption in different spaces of the building.

Zone	Lux
Bedroom 1	100
Bedroom 2	100
Kitchen	200
Hall	200
Bathroom	100
Toilet	100
Staircase and Entrance	150
Parking	150

2025, and the growth in CO_2 pollutants during these 5 years has been calculated. These pollutants are able to be directed in the building space from outside by air conditioning systems and impair air quality. Hence, five design variables are examined to optimize air quality. The design variables are the cooling and heating set point temperature of the air conditioning thermostat, the level of the residents' clothes for the hot and cold seasons and the amount of fresh air that is transferred into the building by the ventilation system. These variables are selected in order to optimize the objective functions of study, which are the amount of CO_2 concentration (to optimize indoor air quality) in the ventilated areas of the building and the annual cost of electricity consumption of the building and thermal comfort. Morris sensitivity analysis was used to investigate the effect of 5 design variables on the three objective functions. In order to have the desired air quality and economic costs for the building, as well as the thermal comfort of the building occupants, all three objective functions must be minimized at the same time. Therefore, design variables and objective functions in JEPLUS software are designed, and at the next step, they are analyzed based on the building's energy performance using EnergyPlus software. The elicited data are then transferred to JEPLUS + EA software, where they are optimized by the NSGA-II algorithm. This algorithm determines the most optimal states so that users can select any state that is in line with their goals. To select the optimal point, the weighted average method is applied so that all three objective functions are reduced to the desired level.

2. Materials and methods

2.1. Weather stations

In this article, 6 cities from 6 different states of the U.S are selected according to the continental division of the United States (Abichou et al., 2015). These 6 cities are chosen based on having different climates. For instance, Cold Bay, Alaska is opted as it owns a polar and very cold climate, and Rogers, Oklahoma is the targeted city that represents a humid continental climate, The rest of the cities were selected based on having different climatic characteristics. Owing to the fact that the United States has variety in climatic conditions and does not have a unified climate like other countries, this variety is expected to affect the energy consumption of buildings and causes the amounts of pollutants and their emissions to be different for each climatic condition. For this reason, American cities are chosen to be analyzed in present study. The climatic and geographical specifications of each city can be seen in Fig. 1 and Table 1.

2.2. Buildings and materials

In recent years, the models used by researchers are based on the characteristics of a real building, and in this article, we have tried to use the same model and the characteristics of a real building have been modeled (Naderi et al., 2020; Baghoolizadeh et al., 2021; Solgi et al., 2018; Ahangari and Maerefat, 2019; Muruganantham, 2010; Refat and Sajjad, 2020; Alghoul, 2017). This is useful because the calculations of a real building in the city can be done accurately enough. After all, the characteristics of the building get closer and closer to the real state. For example, a residential building is adjacent to other buildings in different directions, and the building spaces are designed and built to prevent energy loss. This residential building is adjacent to neighboring buildings in the directions of east and west. The building consists of four floors, of which the lower floor is the parking lot and the upper three floors are the residential type that has similar plans. Each floor includes two bedrooms, a bathroom, a kitchen, and a living room. For the bedrooms on the north side of the building, a window is considered to receive sunlight and affect the energy of the building. The shape of the residential building and the specifications of the residential floor spaces are shown in Fig. 2 and Table 2 (see Fig. 3).

Although energy consumption in buildings varies in different climatic conditions, many studies have shown that a building with unique coverage and air conditioning systems can be used for different climates (Naderi et al., 2020; Baghoolizadeh et al., 2021; Solgi et al., 2018; Ahangari and Maerefat, 2019; Muruganantham, 2010; Refat and Sajjad, 2020; Alghoul, 2017).

Buildings' Covering is one of the effective factors in preventing energy loss. In most previous studies, researchers considered transparent and opaque building materials to be the same for different climates to provide the same conditions for the simulations (Baghoolizadeh et al., 2021; Foroughi et al., 2021; Huo et al., 2021; Synnefa et al., 2007). The U values (Total heat transfer coefficient) of materials in the building envelope (opaque materials) are summarized according to Table 3 and the building windows (transparent materials) have clear double-glazed glass with a thickness of 6 mm and an air layer of 13 mm between, the optical properties of which are shown in Table 4.

2.3. HVAC system and internal gain loads

A proper air conditioning system in the building can affect the energy consumption of the building. The packaged terminal heat pump system, or PTHP for short, is one of the systems that researchers have used experimentally and in the simulated form in their studies (Naderi et al., 2020; Muruganantham, 2010; Refat and Sajjad, 2020; Alghoul, 2017; Wiryadinata et al., 2016). In this study, a packaged terminal heat

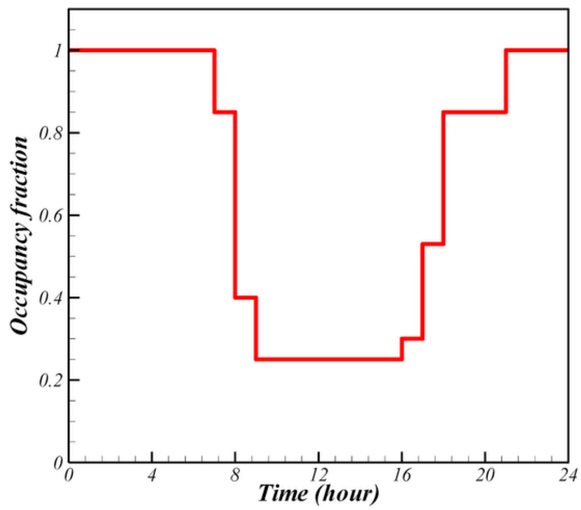

Fig. 4. Occupancy fraction for the model.

Table 7
Electricity consumption costs for different US states.

State	Average Price of Electricity (**Cents/kWh**)
Alaska	23.99
Colorado	12.84
Florida	11.71
Utah	11.09
Kentucky	10.55
Oklahoma	10.11

pump (PTHP) as the air conditioning system is applied to heat and cool the building. This system has two direct expansion coils, one for cooling (cooling coil (DX) and the other for space heating (heating coil) (DX). This system can employ electricity for cooling and gas or electricity for heating. In this study, the air conditioning system uses electricity for both cooling and heating and also uses a fan to direct the hot or cold air to the desired space, regulate the pressure and clean the indoor air. Another privilege of this system is, on the one hand, bringing fresh air into its cycle, and removing the circulating air in the space on the other hand. Due to the residential nature of the building, the thermostat temperature is 22 °C for heating and 25 °C for constant cooling. Fig. 2 and Table 5 describe the specifications of the ventilation system.

For the internal loads of the building, 4 individuals are considered for each floor, and for lighting, a fluorescent lamp is utilized in each room, the electricity consumption (per unit of lux) of which is described in Table 6. Also, the amount of 1000 W is considered for electrical appliances. The schedule of occupancy level is shown in Fig. 4.

2.4. Electricity costs

According to the US Department of Energy (www.eia.gov.), the cost of electricity consumption is determined for each state, which is described in Table 7.

2.5. Group method of data handling (GMDH) neural network

Neural networks have shown to be a reliable and accurate tool for researchers to analyze and predict results (Ivakhnenko, 1971; Rustamovich Sultanbekov et al., 2020; Srinivasan, 2008), one type of which is the group method of data handling (GMDH) neural networks. Ivakhnenko (1971) first developed this type of neural network in 1971. This type of neural network has been used in various fields of engineering (Zhang et al., 2022; Nabipour et al., 2020; Shahsavar et al., 2019; Loni et al., 2018; Lin et al., 2022; Xie and Sun, 2022; Wang et al., 2022; Zor et al., 2020; Rostamzadeh-Renani et al., 2022; Madandoust et al., 2010). The technique of this type of neural network is to use the approach of self-organization and automatic optimization that receives a large number of inputs and delivers one output. This type of neural network can be used in many ways, including predicting, optimizing, modeling complex systems, data mining, etc. The main purpose of the GMDH neural network is to create and predict meaningful output data. GMDH owns three general layers of the input layer, the hidden layer, and the output layer. The inputs combine as compounds $\binom{n}{2}$ to form a neuron, each of which contains a polynomial equation. In the same way, the neurons are combined to reach the final layer or output layer. In the GMDH type of artificial neural network, the input function is X and the output value is y. The approximate output value predicted by the neural network is shown with $\widehat{y}$ and $\widehat{f}$ is the approximate function for f. In multi-input functions of M and single output function of n, the actual values are obtained according to Eq. (1).

$$y = f\left(x_{i1}, x_{i2}, x_{i3}, \ldots, x_{in}\right)\ (i = 1, 2, 3, \ldots, M) \tag{1}$$

The values of $\widehat{y}$ are predicted by the function $\widehat{f}$ with the input vector of $X = \left(x_{i1}, x_{i2}, x_{i3}, \ldots, x_{in}\right)$ and their relation is according to Eq. (2),

$$\widehat{y}_i = \widehat{f}\left(x_{i1}, x_{i2}, x_{i3}, \ldots, x_{in}\right)\ (i = 1, 2, 3, \ldots, M) \tag{2}$$

In the next step, it is demanded to calculate the number of error squares between the output and the output approximated by GMDH, which must be minimized. The equation of the least-squares of error between these two outputs is calculated according to Eq. (3),

$$\sum_{i=1}^{M}\left[\widehat{f}\left(x_{i1}, x_{i2}, x_{i3}, \ldots, x_{in}\right) - \widehat{y}_i\right]^2 \quad \to \min \tag{3}$$

The inputs and the outputs are related by the famous Volttera series (Farlow, 1984) according to Eq. (4),

$$\begin{aligned} y = a_0 + \sum_{i=1}^{n} a_i x_i + \sum_{i=1}^{n}\sum_{j=1}^{n} a_{ij} x_i x_j \\ + \sum_{i=1}^{n}\sum_{j=1}^{n}\sum_{k=1}^{n} a_{ijk} x_i x_j x_{k+} \ldots \end{aligned} \tag{4}$$

The polynomials in Eq. (4) are regulated by Kolmogorov-Gabor (Ivakhnenko, 1971; Farlow, 1984; Sanchez et al., 1997) polynomials as explained in Eq. (5),

$$\begin{aligned} \widehat{y} &= G\left(x_i, x_j\right) \\ &= c_0 + c_1 x_i + c_2 x_j + c_3 x_i^2 + c_4 x_j^2 + c_5 x_i x_j \end{aligned} \tag{5}$$

Eqs. 1 and 2 are described by Eq. (6), which must be minimized,

$$E = \frac{\sum_i^M \left(y_i - G_i\right)^2}{M} \longrightarrow \min \tag{6}$$

In the GMDH algorithm, all probabilities of two variables independent of the sum of n input variables are considered for regression construction. The polynomial in the form of Eq. (6) which best corresponds to the dependent observations is the first hidden layer of the feed-forward neuron network ($\binom{n}{2} = \frac{n(n-1)}{2}$ of $y_i(i = 1,2, \ldots,M)$) that means the least squares. As a result, M can be the number of observations $\left\{\left(y_i, x_{ip}, x_{iq}\right); (i = 1, 2, 3, \ldots, M)\right\}$ for different p,$q \in$ {1,2,3, …,n} acquired and using the polynomial equation of Eq. (5) in addition to

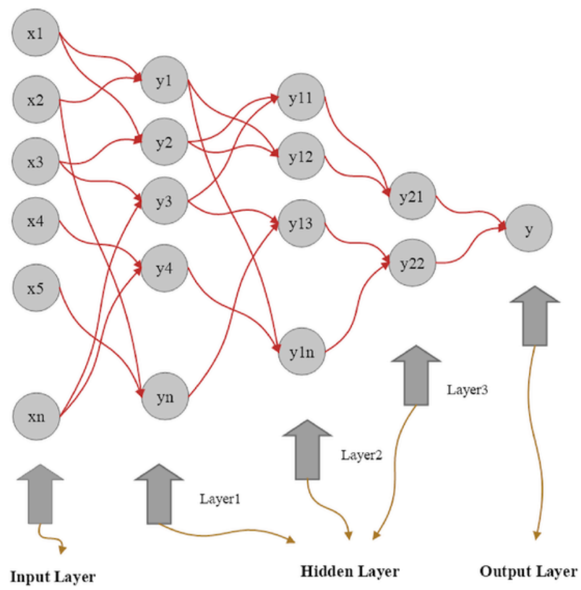

Fig. 5. The formation of neurons in each layer.

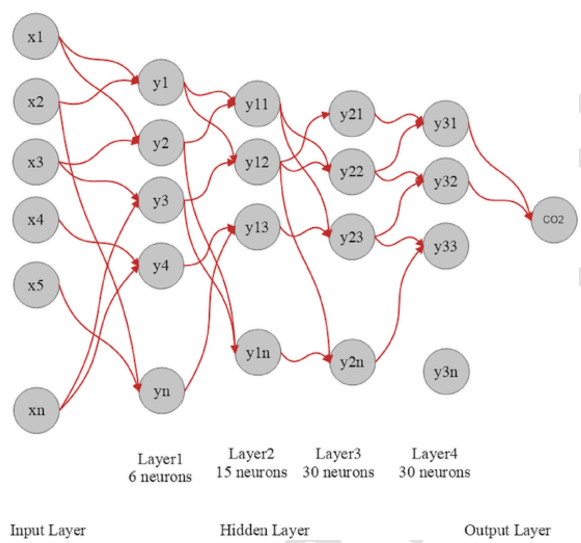

Fig. 6. The positioning of neural network neurons to predict CO_2 concentration.

$\begin{bmatrix} x_{1p} & x_{1q} & \vdots & y_1 \\ x_{2p} & x_{2q} & \vdots & y_2 \\ \cdots & \cdots & \vdots & \cdots \\ x_{Mp} & x_{Mq} & \vdots & y_M \end{bmatrix}$, the matrix equation can be written for each triple row M according to Eqs. (7)–(9),

$$Ac = y \tag{7}$$

$$c = \{c_0, c_1, c_2, c_3, c_4, c_5\} \tag{8}$$

$$y = \{y_1, y_2, y_3, \dots, y_M\}^T \tag{9}$$

The matrix A is then changed to Eq. (10),

$$A = \begin{bmatrix} 1 & x_{1p} & x_{1q} & x_{1p}x_{1q} & x_{1p}^2 & x_{1q}^2 \\ 1 & x_{2p} & x_{2q} & x_{2p}x_{2q} & x_{2p}^2 & x_{2q}^2 \\ \cdots & \cdots & \cdots & \cdots & \cdots & \cdots \\ 1 & x_{Mp} & x_{Mq} & x_{Mp}x_{Mq} & x_{Mp}^2 & x_{Mq}^2 \end{bmatrix} \tag{10}$$

The matrix c is eventually calculated according to Eq. (11),

$$c = \left(A^T A\right)^{-1} A^T y \tag{11}$$

The optimal values of the coefficients of Eq. (5) (Kolmogorov-Gabor polynomials) is calculated through Eq. (11). In Eq. (11), the A is a matrix that can be obtained through Eq. (10) and A^T is the matrix transpose of A. This process is performed again for all the next neurons of the hidden layer which are associated with the configuration of the neural network connection. Fig. 5 shows the schematic for the formation of neurons in the layers.

2.6. *Time series prediction by GMDH*

There are several methods for predicting time series. A classic method for predicting time series is to use latency or previous data $(y_{t-1}, y_{t-2}, y_{t-3}, \dots, y_{t-d})$ where d is the number of delays and y_t is the output and the function of y_t is in the form of Eq. (12),

$$y_t = f\left(y_{t-1}, y_{t-2}, y_{t-3}, \dots, y_{t-d}\right) \tag{12}$$

There is no systematic method for determining the value of d. However, two methods of *adhoc* and Box Jenkins (Shabri and Samsudin, 2014) can be taken into consideration. The delays obtained from the Box Jenkins method are very important for the input layer of the GMDH neural network. This is how the GMDH neural network makes time-series predictions. There are two criteria for evaluating the neural network model, one is R^2 and the other is RMSE (root mean square error) which are described as Eq. (13) and Eq. (14). The closer the value of R^2 is to one and the closer the value of RMSE is to zero, the closer the predicted points of the neural network are to the simulation points.

$$R^2 = 1 - \sum_{i=1}^{n} \frac{\left(y_{i,ANN} - y_{i,Simulation}\right)^2}{y_{i,Simulation}^2} \tag{13}$$

$$RMSE = \sqrt{\frac{\sum_{i=1}^{n}\left(y_{i,ANN} - y_{i,Simulation}\right)^2}{n}} \tag{14}$$

2.7. *Morris sensitivity analysis*

Researchers use sensitivity analysis to study the effect of input variables on output variables. There are several methods for sensitivity analysis, one of which is Morris sensitivity analysis (www.eia.gov.). Morris sensitivity analysis (Morris, 1991) is a so-called one-time-at-one-time (OAT) method, meaning that only one input parameter is given a new value per run. In this method, the parameter f is first considered as an independent input with k, which means that $X = (X_1, X_2, \dots, X_n)$ in the next k space Ω^k $(\Omega^k \subset \mathscr{R}^k)$ are definable. Y is also considered as the output of the model in question, with $Y = f(X)$ in addition to the value of X being attributed to Ω^k or $X \in \Omega^k$. If the value of X_i changes with Δ while the values of all other inputs remain unchanged, the output is $f(X_1, \dots, X_{i-1}, X_i + \Delta, X_{i+1}, \dots, X_k)$ considering $(X_1, \dots, X_{i-1}, X_i + \Delta, X_{i+1}, \dots, X_k) \in \Omega^k$. EE_i can be calculated according to Equation (15).

$$EE_i = \frac{f\left(X_1, \dots, X_{i-1}, X_i + \Delta, X_{i+1}, \dots, X_k\right) - f(X)}{\Delta} \tag{15}$$

Equation (15) follows the OAT method. In Morris Sensitivity Analysis (Morris, 1991), mean deviation and standard deviation, known as μ and σ, respectively, are used as the screening criteria and are calculated according to Equations 16 and 17.

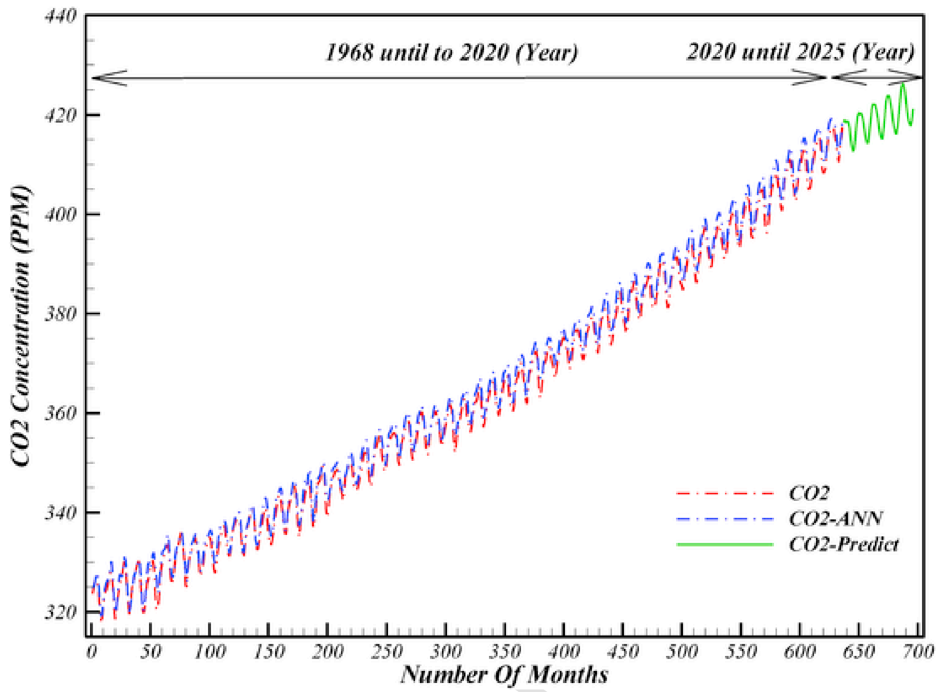

Fig. 7. Predicted CO_2 concentration levels from 2020 to 2025.

Table 8
Values obtained from R^2 and RMSE for the objective function.

Objective	RMSE	R^2
CO_2 concentration	0.87	0.985552

$$\mu_i = \frac{1}{N}\sum_{r=1}^{n} EE_{i,r} \tag{16}$$

$$\sigma_i = \sqrt{\frac{1}{N-1}\sum_{r=1}^{n}\left(EE_{i,r} - \mu_i\right)^2} \tag{17}$$

According to Equations 16 and 17, the higher the value of μ is, the greater the effect of the input parameter on the output is. Moreover, if the value of σ becomes higher, the interaction of the input parameter with other parameters enhances.

2.8. Predicting CO_2 concentration

One of the long-standing environmental problems has long been the presence of pollutants. With the development of cities and the increase in human population, the construction of residential and commercial buildings has increased rapidly and the activity of power plants has doubled to supply their energy consumption. Humans also use energy carriers for transportation in their daily lives. All of these factors have led to a sharp rise in environmental pollutants, including CO_2. The increase of pollutants, it has caused global warming, which in turn has resulted in climate change. CO_2 data are recorded annually by the Global Monitoring Laboratory (https://gml.noaa.gov/.), the latest of which is available for 2020. The purpose of this paper is to predict the amount of CO_2 pollutants in the coming years. In this paper, using time series prediction by GMDH neural network, CO_2 emission values are predicted by 2025 for 6 American cities. The GMDH type of artificial neural network can predict the amount of CO_2. To predict the amount of CO_2 pollutants for the coming year, the recorded data regarding the amount CO_2 pollutants in previous years are integrated. Fig. 6 shows how the neurons combine and is located in each layer. Moreover, the predicted amounts of CO_2 for Niwot Ridge, the values of RMSE and R^2 and the scattering of data is shown in Fig. 7, Table 8 and Fig. 8, respectively.

According to Fig. 7, the amount of CO_2 will increase significantly during 5 years (2020–2025) as is expected. Fig. 7 and Table 8 were related to Niwot Ridge. The results for other cities are fully described in the appendix. The percentage of CO_2 increase can also be seen in Table 9 for each city monthly.

Table 9 shows that the amount of CO_2 would increase by 1–3% in the next 5 years which is a matter of concern for human society and causes deleterious consequences for human health. One of these problems is related to the residential buildings sector, which makes unfavorable air quality inside the building. Air conditioning systems use outside air to cool and heat the building, and because of their mechanism, they make the air temperature favorable for the residents and transfer it to the spaces by the fan. Residents also emit CO_2 as a result of daily activities and respiration. All these factors reduce the desired quality of indoor air and increase CO_2 inside the building and subsequently decrease the oxygen in the air which causes dizziness and headaches in residents. The purpose of the present research is to improve indoor air quality along with reducing the annual cost of electricity consumption of the building, which is fully described in the following parts.

2.9. Design variables and objective functions

EnergyPlus is one of the most powerful software in the field of energy and building. The software was developed by the US Department of Energy and all parts were tested experimentally before it was released (Tabares-Velasco et al., 2012; Mateus et al., 2014; Pereira et al., 2014; Henninger et al., 2004). This software is used by researchers in various fields of energy and building (Naderi et al., 2020; Pandey et al., 2021; Kamal et al., 2019). Yi Zhang (Mashrae) first introduced *jEPlus* software in 2012 as the parameterization tool for EnergyPlus. This software is one of the most powerful software in the field of parameterization that is paired with energy software and design parameters can be set numerically or categorically for it (Zhang and Korolija, 2010; Naboni et al., 2013). Zhang then introduced another software called *jEPlus + EA* to improve the capabilities of the software which were the

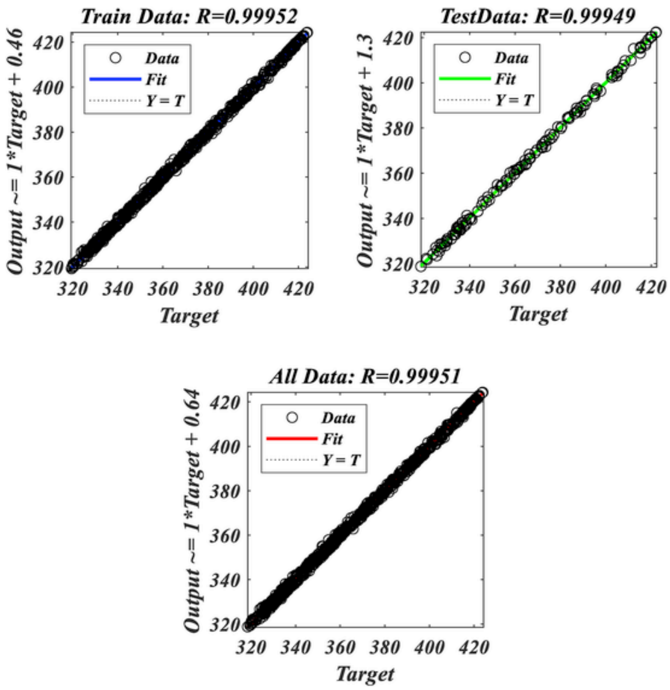

Fig. 8. Dispersion of CO_2 concentration data.

possibility for conducting optimization (NSGAII) (Said et al., 2021; Naderi et al., 2020; Delgarm et al., 2016a), sensitivity analysis (Naji et al., 2021; Delgarm et al., 2018; Chen and Tsay, 2021) and a variety of random sampling methods (Said et al., 2021; Chen and Tsay, 2021; Guo et al., 2019). The design variables of the present study are the heating and cooling set point temperature of the thermostat, clothing insulation value (CLO) (ANSI/ASHRAE, 2013), and the amount of fresh air (ASHRAE 62.1 and V.f.a.i.a.q, 2016) that is transferred into the building by the air conditioning system. The objective functions are the amount of CO_2 concentration inside the building, the building's annual cost of electricity consumption and the occupants' thermal comfort that are targeted to concurrently be reduced. The design variables designed in *jEPlus* software can be seen in Table 10.

Changes in the clothing insulation level of the residents in the cold and hot seasons affect their thermal comfort. This thermal comfort can also be provided with heating and cooling set point thermostat temperatures. Hence, with the proper design of these four parameters, the annual electricity cost can be diminished and the desired thermal comfort for the residents can be provided. As the amount of fresh air inside the spaces increases, the air quality is affected inside the building. On the other hand, the annual electricity consumption of the building increases. Therefore, the amount of fresh air should be set to optimize the amount of CO_2 concentration and the annual electricity consumption of the building. Statistical analysis such as Morris sensitivity analysis can be used to show the effect of design variables on objective functions. Table 11 shows the sampled results of the Morris sensitivity analysis (Morris, 1991) for the objective functions and design variables.

After examining the effect of design variables on objective functions, it is crucial to discover the most optimal points that minimize all three objective functions. Parametric variables that are parametrized by JEPLUS software must be transferred to JEPLUS + EA software for optimization. In JEPLUS + EA software, the parametric variables are optimized using genetic algorithm. The schematic of the energy simulation to optimization process is detailed in Fig. 9.

2.10. *Multi-objective optimization of the building's annual electricity consumption cost and CO_2 concentration and thermal comfort*

In this study, it is targeted to reduce the electricity consumption cost of the building as well as improving indoor air quality and thermal comfort of residents. In recent years, researchers have focused their studies on the feasible methods of diminishing the energy consumption of buildings. Due to the fact that fossil fuels are burned to generate electricity in power plants, the role of household's energy reduction is becoming more prominent to minimize the utilization of fossil fuels. With global increase in the electricity consumption and burning of fossil resources, various pollutants are released into the environment and endanger human life. Polluted air is transported inside the building using mechanical or natural ventilation, which reduces the quality of indoor air, which subsequently endangers the health condition of residents. Also, in the buildings, conditions should be provided for the residents to benefit from high heating comfort. In order to accomplish these goals, a multi-objective optimization must be performed. Researchers have faced great challenges in selecting the right optimization algorithms and have used different optimization algorithms for their simulated results as needed to achieve optimal choices for their research. One of the most common algorithms for optimization purposes is the genetic algorithm (Li et al., 2021). One of the most well-known algorithms in the field of multi-objective optimization is the Non-Dominant Genetic Algorithm (NSGA), the second version of which was introduced as NSGA-II in 2002 (Deb et al., 2002). This algorithm was used in various fields of energy and buildings (Bre et al., 2016; Carlucci et al., 2015; Rosso et al., 2020; Yang et al., 2016). Since there are no restrictions on the selection of continuous and discrete decision variables in this algorithm, NSGA-II is used as an optimization method in present research. Furthermore, since most optimization problems have more than one objective function and the objective functions are usually in conflict with each other, it offers a set of solutions that are not superior to each other, which is called the Pareto front (Asadi et al., 2012; Zhai et al., 2019). In this study, JEPLUS + EA software is implemented for multi-objective optimization (Zhang, 2012). JEPLUS + EA software requires JEPLUS parameterized data. For this purpose, in JEPLUS software, the weather data and the simulated data are inserted as the input for this software. Then, the design variables are created in JEPLUS software and used as the inputs to reach the objective functions. The file created by JEPLUS is now transferred to JEPLUS + EA. Due to the fact that the modes of the design variables interact with each other alternately, it will face a very large number of modes. As a result, the NSGA-II algorithm is used to lead the model to the best points or Pareto front. For the configuration of the algorithm with the initial analysis performed for convergence, population size, maximum number of generations, crossover rate and mutation rate are considered 10, 50, 100% and 20%, respectively. After performing the optimization and receiving the Pareto front from the NSGA-II algorithm, the best point is required to be selected. There are many statistical methods for reaching the best possible answer. One of the applicable methods that is commonly employed by many researchers (Delgarm et al., 2016b; Karmellos et al., 2015; Ryu et al., 2009) is the sum of weighted method. This method estimates the best answer using Equation (18).

$$f_{ws}(x) = \sum_{i=1}^{n} a_i \frac{f_i(x) - f_i(x)^{min}}{f_i(x)^{max} - f_i(x)^{min}} \tag{18}$$

Where $f_i(x)$ are the objective functions, ie power consumption, thermal and visual comfort, and similarly $f_i(x)^{min}$ and $f_i(x)^{max}$ are the minimum and maximum of each objective function.a_i is the weight coefficient. It means that considering that thermal comfort and co2 concentration are of equal importance, the value of the weight coefficient of these two functions is assumed to be the same. Therefore, the weight coefficient can be calculated according to Equation (19).

Table 9
Monthly increase in CO_2 concentration during 5 years from 2020 for the cities of (a) Cold Bay (b) Niwot Ridge (c) Key Biscayne (d) Midway (e) Rogers (f) Wendover.

(a)

Annual	4978.2	5003.03	0.5	4978.2	5023.75	0.915	4978.2	5027.81	0.997	4978.2	5048.12	1.405	4978.2	5067.65	1.797
Dec	419.8	421.135	0.318	419.8	422.433	0.627	419.8	422.845	0.725	419.8	424.450	1.108	419.8	425.7	1.4
Nov	417.5	418.85	0.323	417.5	420.238	0.656	417.5	420.089	0.62	417.5	420.933	0.822	417.5	421.9	1.05
Oct	414	415.464	0.354	414	416.363	0.571	414	415.212	0.293	414	416.031	0.491	414	417.2	0.77
Sep	407.3	408.939	0.402	407.3	411.114	0.936	407.3	411.756	1.094	407.3	412.553	1.289	407.3	414.3	1.73
Aug	402.8	406.324	0.875	402.8	409.411	1.641	402.8	409.617	1.692	402.8	411.159	2.075	402.8	413.6	2.67
Jul	406.1	409.266	0.78	406.1	411.796	1.403	406.1	412.617	1.605	406.1	415.433	2.3	406.1	417.8	2.88
Jun	414.1	416.623	0.609	414.1	418.677	1.105	414.1	418.986	1.18	414.1	420.813	1.621	414.1	422.7	1.75
May	418.8	420.921	0.506	418.8	422.358	0.85	418.8	422.789	0.952	418.8	424.435	1.346	418.8	426.1	1.75
Apr	419.9	421.988	0.497	419.9	423.517	0.861	419.9	424.140	1.01	419.9	425.739	1.391	419.9	427.4	1.79
Mar	420.5	422.259	0.418	420.5	423.631	0.745	420.5	424.982	1.066	420.5	426.177	1.35	420.5	427.6	1.69
Feb	419.6	421.255	0.394	419.6	422.415	0.671	419.6	423.748	0.989	419.6	425.497	1.405	419.6	427	1.76
Jan	417.8	420	0.526	417.8	421.796	0.956	417.8	423.025	1.251	417.8	424.900	1.7	417.8	426.3	2.03
Year	2020 (ppm)	2021 (ppm)	Increase (%)	2020 (ppm)	2022 (ppm)	Increase (%)	2020 (ppm)	2023 (ppm)	Increase (%)	2020 (ppm)	2024 (ppm)	Increase (%)	2020 (ppm)	2025 (ppm)	Increase (%)

(b)

Annual	4980.68	4998.68	0.361	4980.68	5014.63	0.682	4980.68	5029.62	0.983	4980.68	5043.25	1.256	4980.68	5064.30	1.679
Dec	417.490	417.791	0.072	417.490	418.850	0.326	417.490	419.626	0.512	417.490	420.281	0.668	417.490	421.202	0.89
Nov	414.940	415.366	0.103	414.940	416.489	0.373	414.940	417.307	0.570	414.940	417.833	0.697	414.940	418.901	0.955
Oct	412.430	413.043	0.149	412.430	414.386	0.474	412.430	415.262	0.687	412.430	416.213	0.917	412.430	417.848	1.314
Sep	410.450	412.634	0.532	410.450	414.291	0.936	410.450	415.260	1.172	410.450	416.328	1.432	410.450	418.141	1.874
Aug	411.720	413.620	0.461	411.720	415.216	0.849	411.720	416.330	1.120	411.720	417.287	1.352	411.720	419.061	1.784
Jul	413.850	415.426	0.381	413.850	416.686	0.685	413.850	417.902	0.979	413.850	418.830	1.203	413.850	420.701	1.656
Jun	415.410	417.547	0.514	415.410	418.503	0.745	415.410	419.617	1.013	415.410	420.786	1.294	415.410	422.824	1.785
May	417.130	418.646	0.364	417.130	419.719	0.621	417.130	420.916	0.908	417.130	422.291	1.237	417.130	424.849	1.851
Apr	417.540	418.709	0.280	417.540	420.285	0.658	417.540	422.021	1.073	417.540	423.604	1.452	417.540	426.135	2.059
Mar	417.200	418.401	0.288	417.200	420.072	0.688	417.200	422.007	1.152	417.200	423.894	1.605	417.200	426.240	2.167
Feb	416.840	418.974	0.512	416.840	420.375	0.848	416.840	422.138	1.271	416.840	423.604	1.623	416.840	425.262	2.02
Jan	415.680	418.526	0.685	415.680	419.766	0.983	415.680	421.242	1.338	415.680	422.303	1.593	415.680	423.139	1.794
Year	2020 (ppm)	2021 (ppm)	Increase (%)	2020 (ppm)	2022 (ppm)	Increase (%)	2020 (ppm)	2023 (ppm)	Increase (%)	2020 (ppm)	2024 (ppm)	Increase (%)	2020 (ppm)	2025 (ppm)	Increase (%)

(c)

Annual	4981.84	5005	0.465	4981.84	5020.87	0.783	4981.84	5037.73	1.122	4981.84	5052.32	1.415	4981.84	5066.54	1.7
Dec	415.320	418.186	0.690	415.320	419.025	0.892	415.320	419.939	1.112	415.320	421.488	1.485	415.320	422.916	1.829
Nov	415.860	417.637	0.427	415.860	419.205	0.804	415.860	420.407	1.093	415.860	421.671	1.397	415.860	422.942	1.703
Oct	417.230	419.167	0.464	417.230	419.688	0.589	417.230	420.533	0.792	417.230	421.586	1.044	417.230	422.929	1.366
Sep	419.330	419.690	0.086	419.330	419.971	0.153	419.330	421.121	0.427	419.330	422.031	0.644	419.330	423.067	0.891
Aug	418.520	419.712	0.285	418.520	421.603	0.737	418.520	422.161	0.870	418.520	423.000	1.070	418.520	423.696	1.237
Jul	416.730	419.416	0.644	416.730	421.430	1.128	416.730	422.030	1.272	416.730	423.231	1.560	416.730	424.231	1.800
Jun	414.240	417.291	0.737	414.240	418.972	1.142	414.240	421.211	1.683	414.240	422.988	2.112	414.240	424.393	2.451
May	411.380	414.335	0.718	411.380	416.398	1.220	411.380	419.326	1.931	411.380	421.011	2.341	411.380	422.999	2.824
Apr	409.980	412.721	0.669	409.980	414.037	0.990	409.980	416.565	1.606	409.980	418.247	2.016	409.980	420.345	2.528
Mar	411.680	412.911	0.299	411.680	414.578	0.704	411.680	416.111	1.076	411.680	417.067	1.308	411.680	418.002	1.536
Feb	414.760	416.370	0.388	414.760	417.547	0.672	414.760	418.328	0.860	414.760	419.114	1.050	414.760	419.244	1.081
Jan	416.810	417.572	0.183	416.810	418.416	0.385	416.810	419.988	0.763	416.810	420.876	0.975	416.810	421.771	1.19
Year	2020 (ppm)	2021 (ppm)	Increase (%)	2020 (ppm)	2022 (ppm)	Increase (%)	2020 (ppm)	2023 (ppm)	Increase (%)	2020 (ppm)	2024 (ppm)	Increase (%)	2020 (ppm)	2025 (ppm)	Increase (%)

(d)

Annual	4974.89	4989.93	0.302	4974.89	5007.75	0.661	4974.89	5023.14	0.970	4974.89	5034.413	1.196	4974.89	5047.89	1.467
Dec	415.79	417.549	0.423	415.79	418.638	0.685	415.79	419.830	0.972	415.79	420.424	1.114	415.79	421.389	1.347
Nov	414.72	416.088	0.330	414.72	417.000	0.550	414.72	418.001	0.791	414.72	418.570	0.928	414.72	419.329	1.111
Oct	411.89	412.811	0.224	411.89	414.317	0.589	411.89	415.209	0.806	411.89	416.001	0.998	411.89	416.438	1.104
Sep	409.42	411.177	0.429	409.42	412.850	0.838	409.42	414.194	1.166	409.42	415.196	1.411	409.42	416.098	1.631
Aug	410.43	412.042	0.393	410.43	413.716	0.801	410.43	415.513	1.238	410.43	416.704	1.529	410.43	418.101	1.869
Jul	413.08	414.551	0.356	413.08	416.223	0.761	413.08	418.081	1.211	413.08	419.305	1.507	413.08	420.820	1.874
Jun	415.73	417.337	0.386	415.73	418.969	0.779	415.73	420.516	1.151	415.73	421.514	1.391	415.73	422.835	1.709
May	417.68	419.113	0.343	417.68	420.385	0.648	417.68	421.435	0.899	417.68	422.134	1.066	417.68	423.131	1.305
Apr	417.7	418.490	0.189	417.7	419.773	0.496	417.7	420.776	0.736	417.7	421.593	0.932	417.7	422.846	1.232
Mar	416.81	416.946	0.033	416.81	418.789	0.475	416.81	419.907	0.743	416.81	420.931	0.989	416.81	422.344	1.328
Feb	416.34	416.862	0.125	416.34	418.287	0.468	416.34	419.468	0.751	416.34	420.716	1.051	416.34	422.133	1.391
Jan	415.3	416.965	0.401	415.3	418.806	0.844	415.3	420.214	1.183	415.3	421.326	1.451	415.3	422.428	1.716

(*continued on next page*)

Table 9 (*continued*)

(d)															
Annual	4974.89	4989.93	0.302	4974.89	5007.75	0.661	4974.89	5023.14	0.970	4974.89	5034.413	1.196	4974.89	5047.89	1.467
Year	2020 (ppm)	2021 (ppm)	Increase (%)	2020 (ppm)	2022 (ppm)	Increase (%)	2020 (ppm)	2023 (ppm)	Increase (%)	2020 (ppm)	2024 (ppm)	Increase (%)	2020 (ppm)	2025 (ppm)	Increase (%)
(e)															
Annual	5006.61	5018.88	0.25	5006.61	5034.11	0.55	5006.61	5045.14	0.77	5006.61	5058.29	1.03	5006.61	5069.13	1.25
Dec	423.66	423.749	0.02	423.66	424.39	0.17	423.66	425.69	0.48	423.66	426.20	0.60	423.66	427.38	0.88
Nov	422.14	422.209	0.02	422.14	422.43	0.07	422.14	422.46	0.08	422.14	422.69	0.13	422.14	423.15	0.24
Oct	415.58	415.635	0.01	415.58	415.80	0.05	415.58	415.99	0.10	415.58	416.42	0.20	415.58	416.99	0.34
Sep	412.45	412.753	0.07	412.45	413.87	0.34	412.45	414.58	0.52	412.45	416.21	0.91	412.45	416.87	1.07
Aug	411.96	413.724	0.43	411.96	414.88	0.71	411.96	415.68	0.90	411.96	417.00	1.22	411.96	418.00	1.47
Jul	411.57	414.307	0.66	411.57	416.47	1.19	411.57	417.15	1.35	411.57	418.30	1.63	411.57	419.12	1.83
Jun	415.33	415.986	0.16	415.33	418.13	0.68	415.33	418.82	0.84	415.33	419.37	0.97	415.33	420.28	1.19
May	417.82	417.963	0.03	417.82	418.56	0.18	417.82	419.77	0.47	417.82	420.34	0.60	417.82	421.11	0.79
Apr	417.7	418.483	0.19	417.7	419.41	0.41	417.7	420.57	0.69	417.7	421.61	0.94	417.7	422.61	1.18
Mar	418.14	419.418	0.31	418.14	421.67	0.84	418.14	422.94	1.15	418.14	424.59	1.54	418.14	425.86	1.85
Feb	419.01	420.251	0.30	419.01	422.72	0.89	419.01	424.19	1.24	419.01	426.48	1.78	419.01	427.87	2.11
Jan	421.25	424.413	0.75	421.25	425.78	1.08	421.25	427.32	1.44	421.25	429.09	1.86	421.25	429.90	2.05
Year	2020 (ppm)	2021 (ppm)	Increase (%)	2020 (ppm)	2022 (ppm)	Increase (%)	2020 (ppm)	2023 (ppm)	Increase (%)	2020 (ppm)	2024 (ppm)	Increase (%)	2020 (ppm)	2025 (ppm)	Increase (%)
(f)															
Annual	4980.2	5007.33	0.54	4980.2	5020.18	0.80	4980.2	5031.33	1.03	4980.2	5046.14	1.32	4980.2	5061.35	1.63
Dec	418.86	420.28	0.34	418.86	420.86	0.48	418.86	421.48	0.63	418.86	422.02	0.75	418.86	422.57	0.88
Nov	415.46	417.14	0.40	415.46	417.61	0.52	415.46	417.94	0.60	415.46	418.82	0.81	415.46	419.27	0.92
Oct	412.11	413.53	0.35	412.11	413.91	0.44	412.11	414.81	0.66	412.11	415.98	0.94	412.11	417.52	1.31
Sep	411.28	413.24	0.48	411.28	413.98	0.66	411.28	415.13	0.94	411.28	416.48	1.26	411.28	418.24	1.69
Aug	411.04	413.55	0.61	411.04	414.84	0.92	411.04	416.08	1.22	411.04	417.52	1.58	411.04	419.23	1.99
Jul	411.13	414.56	0.83	411.13	416.14	1.22	411.13	417.42	1.53	411.13	418.86	1.88	411.13	420.38	2.25
Jun	413.31	416.79	0.84	413.31	418.03	1.14	413.31	419.12	1.41	413.31	420.23	1.67	413.31	421.40	1.96
May	416.26	418.42	0.52	416.26	419.39	0.75	416.26	420.34	0.98	416.26	421.43	1.24	416.26	422.49	1.50
Apr	417.37	419.57	0.53	417.37	420.29	0.70	417.37	420.72	0.80	417.37	422.30	1.18	417.37	423.76	1.53
Mar	417.91	419.68	0.42	417.91	420.99	0.74	417.91	421.98	0.97	417.91	423.60	1.36	417.91	425.03	1.70
Feb	418.55	420.31	0.42	418.55	422.11	0.85	418.55	423.22	1.11	418.55	424.91	1.52	418.55	426.24	1.84
Jan	416.92	420.26	0.80	416.92	422.02	1.22	416.92	423.09	1.48	416.92	424.00	1.70	416.92	425.22	1.99
Year	2020 (ppm)	2021 (ppm)	Increase (%)	2020 (ppm)	2022 (ppm)	Increase (%)	2020 (ppm)	2023 (ppm)	Increase (%)	2020 (ppm)	2024 (ppm)	Increase (%)	2020 (ppm)	2025 (ppm)	Increase (%)

Table 10
The properties of the design variables.

Design variables	Unit	Type	Range
Heating Set point	°C	Continuous	(19,22.5)
Cooling Set point	°C	Continuous	(23,26.5)
Summer clothing insulation value	CLO	Continuous	(0.2,0.7)
Winter clothing insulation value	CLO	Continuous	(0.7,1.2)
Fresh Air	$\frac{m^3}{m^2.s}$	Continuous	(0.0003,0.0005)

Table 11
Sensitivity analysis of design variables on objective functions.

Design variables	Objective functions					
	Co2 concentration		Annual electricity consumption cost		PPD	
	μ	σ	μ	σ	μ	σ
Heating Set point	14.48	1.271	919.9	39.91	15.48	5.201
Cooling Set point	4.979	1.745	110.4	29	6.881	4.473
Summer clothing insulation value	0	0	0	0	26.03	6.174
Winter clothing insulation value	0	0	0	0	9.637	3.682
Fresh Air	16.68	1.183	325.5	34.97	0.04698	0.01325

$$a_2 = a_3 = \frac{1 - a_1}{2} \tag{19}$$

Thus, a multi-objective optimization problem became a single-objective optimization problem to determine the coefficient a_1.

3. Results and discussion

After processing the optimization, JEPLUS + EA software provides the Pareto front points to the user. These points are not superior to each other due to the fact that the opposite objective functions are also considered. In other words, when one objective function is in the ideal position, the other two objective functions are not in the desired state. Therefore, a point must be considered that satisfies all the objective functions. As a result, the method of sum of weighted method is used. The weight factor a_1, which is related to annual electricity consumption cost, varies from 0 to 1. According to Equation (19), when a_1 is considered zero, the amount of annual electricity consumed cost is at its maximum state and the other two functions, which are thermal comfort and co2 concentration, are at their lowest. On the other hand, when the value of a_1 is equal to 1, the amount of annual electricity consumption cost is at its minimum state, and the other objective functions are at their highest. In order to select the best point, the value of the weight coefficient, ie a_1, is changed from 0 to 1 in steps of 0.1, and the optimal points are introduced. Then, from the optimal 11 points, a point that can satisfy all the objective functions is selected. The Pareto optimal points for Niwot Ridge are shown in Fig. 10, and the values of the

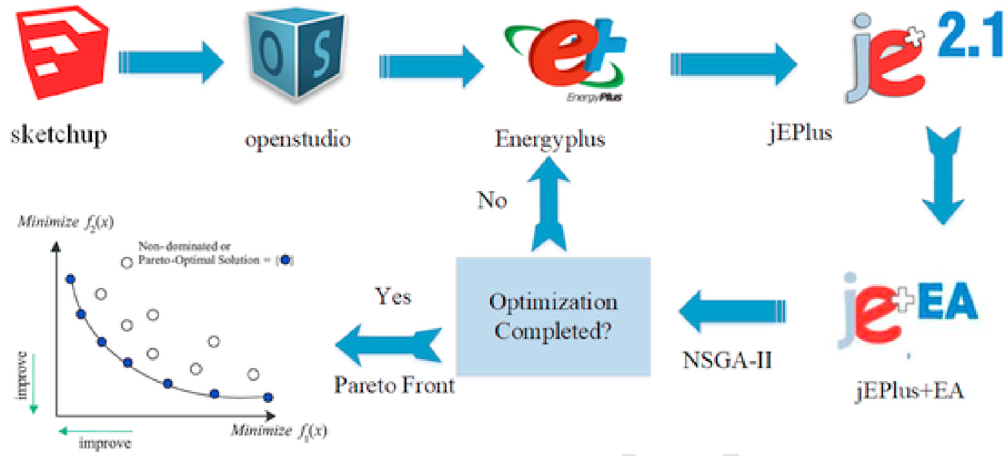

Fig. 9. Schematic of optimization steps.

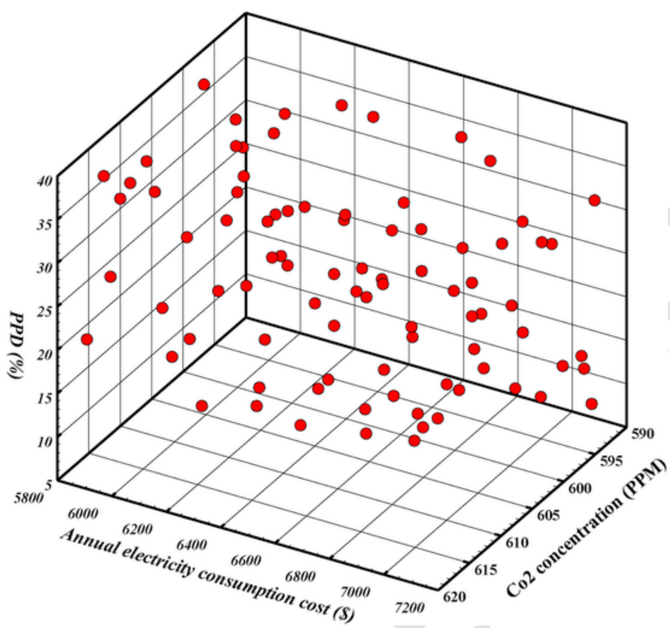

Fig. 10. Optimal points of the Pareto front for Niwot Ridge city.

weight coefficients and selected points of the Pareto front are explained in Table 12.

According to Table 12, when the weight coefficient value is zero, the two objective functions, which are CO2 concentration and thermal comfort, are at their lowest, while the other objective function, which is the annual electricity consumption, is at its maximum. By increasing the weight coefficient, the value of two objective functions that have the same coefficients increases and the value of the other objective function decreases until the value of the weight coefficient reaches 1. This means that the value of the weight coefficient for other two objective functions is zero and omits their effect on the optimal choice. Hence, at this point, the two objective functions are at their maximum, and the third objective function, which is the amount of annual electricity consumption cost, is at its lowest state. Out of these 11 optimal points, it seems that the point with a weight coefficient of 0.5 is optimal because it reduces the two objective functions of annual electricity consumption cost of the building and the amount of CO_2 concentration to a reasonable proportion, and the third objective function, which is the comfort temperature of the occupants, approaches a desired value. According to Table 12 and Fig. 11, increasing the temperature of the heating thermostat causes the amount of annual electricity consumption cost enhances sharply, though the amount of thermal comfort and the amount of CO_2 concentration decreases. Due to the relatively cold weather in Niwot Ridge, when the heating temperature of the thermostat rises, the ventilation system must consume more electricity to bring about the desired room temperature. On the other hand, with increase in electricity consumption, the amount of CO_2 concentration decreases, so a temperature must be chosen that satisfies all three objective functions. The temperature 21.6 °C is the point that favorably optimizes and satisfies the objective functions of the present study. Also, for the thermostat temperature, cooling temperatures above 23.5 °C will satisfy almost all three target functions. Because Niwot Ridge is a cold city, the air conditioning system will produce less chilled air and the higher the temperature of the cooling thermostat is, the less electricity is consumed and the thermal comfort of the residents is fairly desirable. According to Fig. 12, it can be seen that the cooling thermostat tempera-

Table 12
The specifications of optimal points of the Pareto front for Niwot Ridge city.

Coefficient (a_1)	Heating set point (°C)	Cooling set point (°C)	Winter clothing insulation value (CLO)	Summer clothing insulation value (CLO)	Fresh Air $\left(\frac{m^3}{m^2.s}\right)$	CO_2 Concentration (PPM)	Annual electricity consumption cost ($)	PPD (%)
0	22.5	24.4	1.1	0.7	0.00049	595.2	7191.72	10.86
0.1	22.4	25.9	0.85	0.7	0.0005	593.8	7131.31	13.48
0.2	21.7	23.7	1.15	0.7	0.0005	599.2	7003.41	13.45
0.3	22.1	24.5	1.2	0.7	0.00036	608.4	6844.32	11.74
0.4	22.2	26.3	1.1	0.7	0.00031	610.26	6709.93	12.51
0.5	21.6	26.2	1.2	0.7	0.0003	613.41	6541.55	13.92
0.6	20.4	23.1	1.05	0.7	0.00031	622.13	6379.94	20.12
0.7	20	25.9	1.05	0.65	0.00033	616.66	6209	22.88
0.8	19	26.4	1.2	0.5	0.00043	612.39	6100.43	30.93
0.9	19	25.5	1.1	0.3	0.00036	618.68	6036.81	40.51
1	19	25.7	1.1	0.25	0.00033	620.72	5986.91	42.14

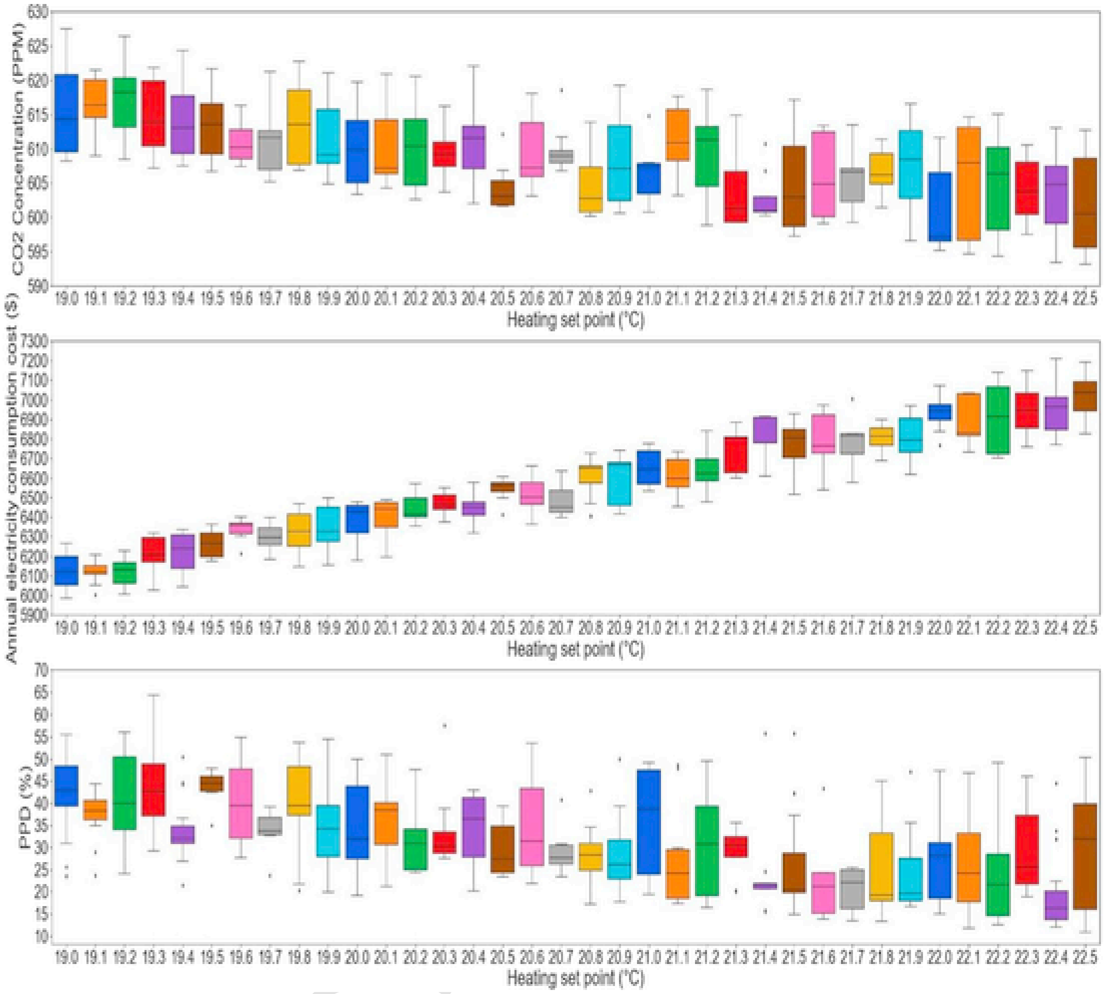

Fig. 11. The effect of heating temperature of thermostat on the objective functions for the city of Niwot Ridge.

ture from a temperature of above 25 °C has a decreasing trend for all three objective functions and the temperature of 26.2 °C results in desirable values for all three objective functions. The amount of clothing level is observed in the warm season. The increase in the clothing level improves the thermal comfort of the building occupants, but has little effect on the other two objective functions. Regarding the clothing level during winter, because the climate of Niwot Ridge is colder than winter, the more clothing level the occupants of the building have, the higher level of thermal comfort can be brought about. The effect of clothing level on the objective functions can be seen in Table 12 and Figs. 13 and 14. The best clothing insulation levels for cooling and heating are 0.7 and 1.2, respectively. According to Table 12 and Fig. 15, increase in the amount of fresh air transferred into the building by the air conditioning system causes the amount of CO_2 concentration inside the building to be reduced, but on the other hand, the amount of electricity consumption cost increases sharply. The reason for this decrease in CO_2 is that the clean air inside the building increases, but on the other hand, the ventilation system must consume more electricity to transfer this amount of air, which subsequently rises electricity consumption cost. On the other hand, the amount of fresh air does not have the same behavior on the thermal comfort of the residents. Based on the sensitivity analysis, indoor air quality has little effect on the thermal comfort of the residents. According to the optimal selection point in Table 12, $0.0003\left(\frac{m^3}{m^2.s}\right)$ fresh air is optimal for Niwot Ridge.

The same procedure is followed to find an optimal point for each city. The optimal point for all cities is given in Table 13.

4. Conclusion

In this paper, the aim was to predict the growth of CO_2 concentration and control its concentration in the building. The amount of CO_2 concentration for 6 cities with different climates was predicted until 2025 and its growth rate was calculated during these 5 years. On the other hand, to control the concentration of CO_2 inside the building, 5 design variables were considered and the goal was to simultaneously reduce the concentration of CO_2 inside the building and the cost of electricity consumption of the building and thermal comfort of residents. According to the results of the present study, the following conclusions can be deduced:

- Using the GMDH artificial neural network time series, the amount of CO_2 concentration from 2020 to 2025 was predicted with high accuracy for 6 cities with different climates. The growth rate of CO_2 during these 5 years was predicted to be between 1 and 3% in all months of the year and 1.25 and 1.8% in the whole year, which in turn will cause concern to human society about its consequences, and measures must be taken to prevent its growth.
- To reduce the concentration of CO_2 in the building space, the best way is to increase the rate of fresh air in the spaces. By appropriately ventilating the air, clean air can be brought into the space and on the other hand, dirty air is removed from the space and provides the desired indoor air quality is provided. Moreover, by increasing the fresh air rate for the entry and exit of the air conditioning system, more electricity is consumed to provide the

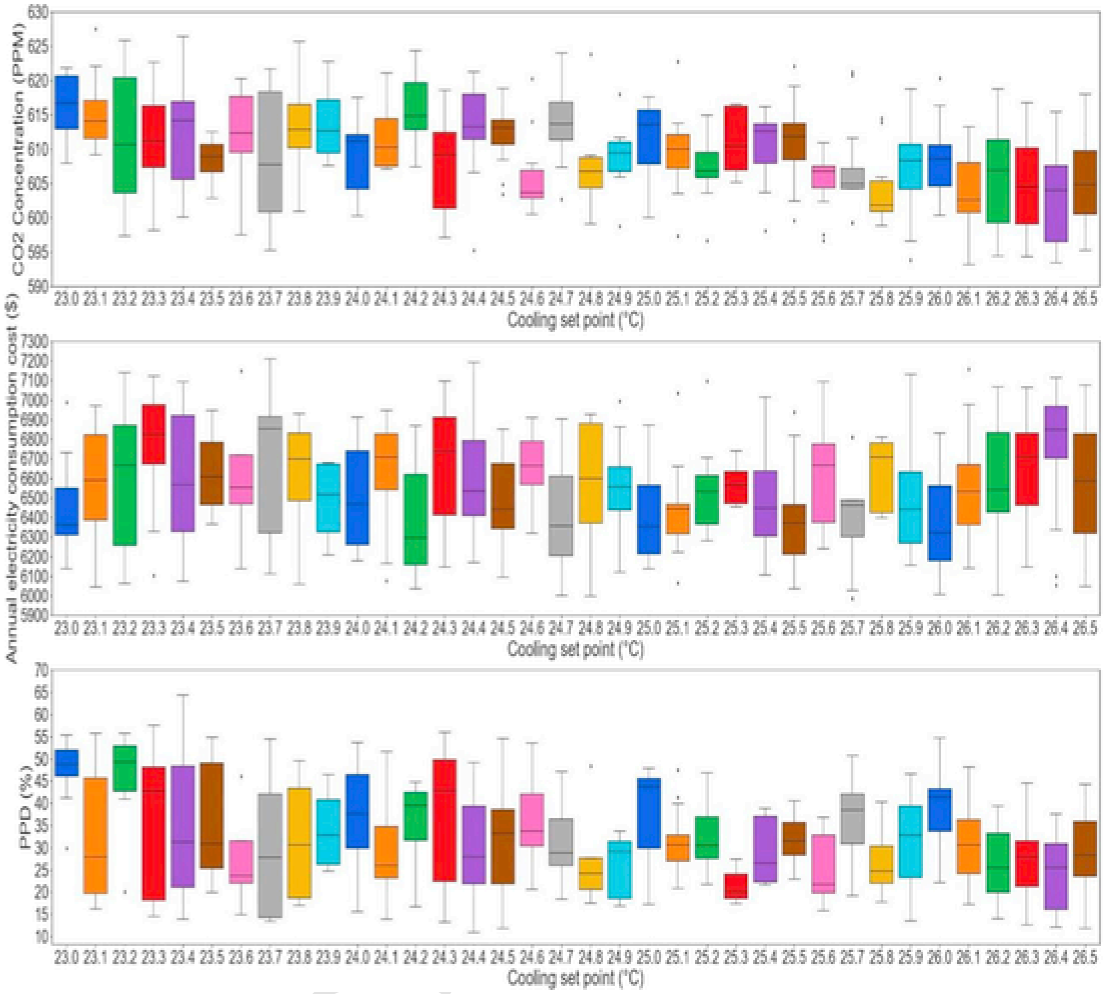

Fig. 12. The effect of cooling temperature of thermostat on the objective functions for the city of Niwot Ridge.

ideal conditions. For this reason, the amount of fresh air through the air conditioning system should be balanced with the ratio of natural air entering the building to efficiently affect the economic costs of the building. Hence, the optimal range of 0.0003–0.0005 $\left(\frac{m^3}{m^2.s}\right)$ for fresh air rates was obtained in six cities with different climates and CO_2 concentrations.

- The clothing insulation level of the residents directly affects the thermal comfort. Thermal comfort can change and be dependent on various factors such as psychological, climatic, etc. For cities whose average temperature reaches below zero in the cold season, higher clothing levels are demanded to provide thermal comfort, and for the warmer seasons, lower clothing levels are needed. Providing thermal comfort reduces the building's electricity consumption, and consequently reduces the economic costs of the building. According to the results of optimizations, the appropriate range of clothing levels for the cold and hot seasons is 0.7–1.2 and 0.55–0.7, respectively.
- The proper cooling and heating set point temperature of the air conditioning system's thermostat reduces both the electricity consumption and building costs. For cities where the temperature is very low in winter, it is optimal to design the thermostat so that the air conditioning system is turned on sooner to heat the building spaces. The proper heating set point temperature of the thermostat is approximately 19 °C for cold cities, and for cities that have a relatively higher temperature, this value reaches between 21 and 22 °C. Similarly, the optimal design values for the cooling set point temperature of the thermostat are between 25 and 26.5.

5. Future study

For future studies, it is suggested that the subject matter of this article be examined experimentally and in field study form by studying several groups of male and female from various age groups. This is due the fact that thermal comfort, in addition to environmental factors, also depends on psychological factors such as gender and people's feeling of coldness and warmness. On the other hand, due to aging and the indication of physical diseases, the immune system and respiratory system of individuals become weak over the time. By increasing the CO_2 and decreasing the oxygen in the space, the possibility of breathing comfortably decreases over time, and it causes headaches and dizziness, which can be partially solved by increasing the fresh air by the air conditioning system. But, the increase of fresh air from the air conditioning system consumes more electricity which imposes higher costs for the residents. Therefore, the fresh air must be transferred to the spaces with an optimal level.

CRediT authorship contribution statement

Mohammadreza Baghoolizadeh : Methodology, Software, Validation, Writing – review & editing, Writing – original draft, Investigation. **Mohammad Rostamzadeh-Renani :** Methodology, Software, Validation, Writing – review & editing, Writing – original draft, Investigation. **Seyed Amir Hossein Hashemi Dehkordi :** Methodology, Software, Validation, Writing – review & editing, Writing – original

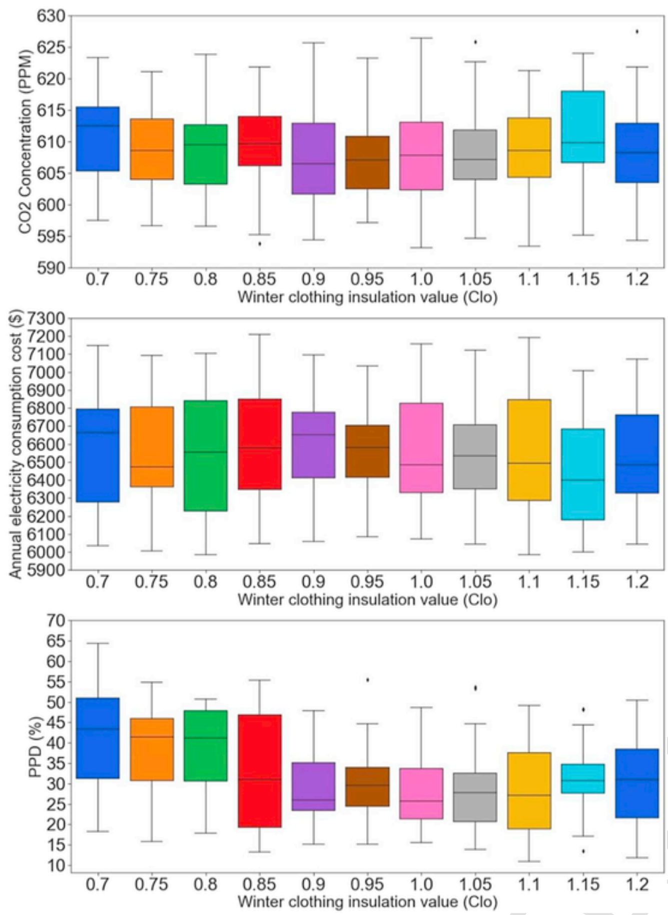

Fig. 13. The effect of winter clothing insulation level on the objective functions for the city of Niwot Ridge.

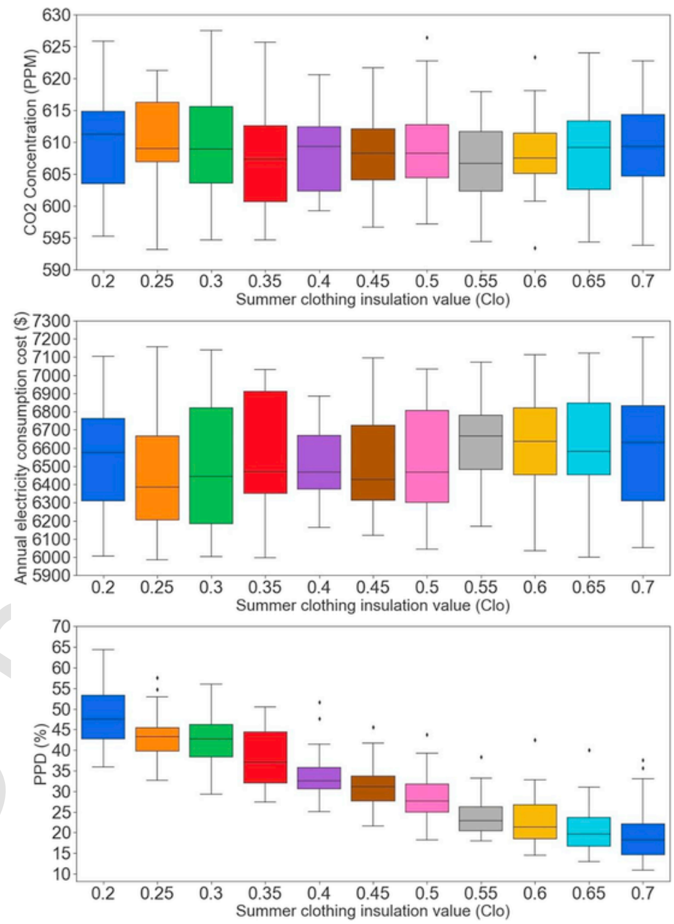

Fig. 14. The effect of summer clothing insulation level on the objective functions for the city of Niwot Ridge.

draft, Investigation. **Reza Rostamzadeh-Renani :** Methodology, Software, Validation, Writing – review & editing, Writing – original draft, Investigation. **Davood Toghraie :** Methodology, Software, Validation, Writing – review & editing, Writing – original draft, Investigation.

Declaration of competing interest

The authors declare that they have no known competing financial interests or personal relationships that could have appeared to influence the work reported in this paper.

Data availability

No data was used for the research described in the article.

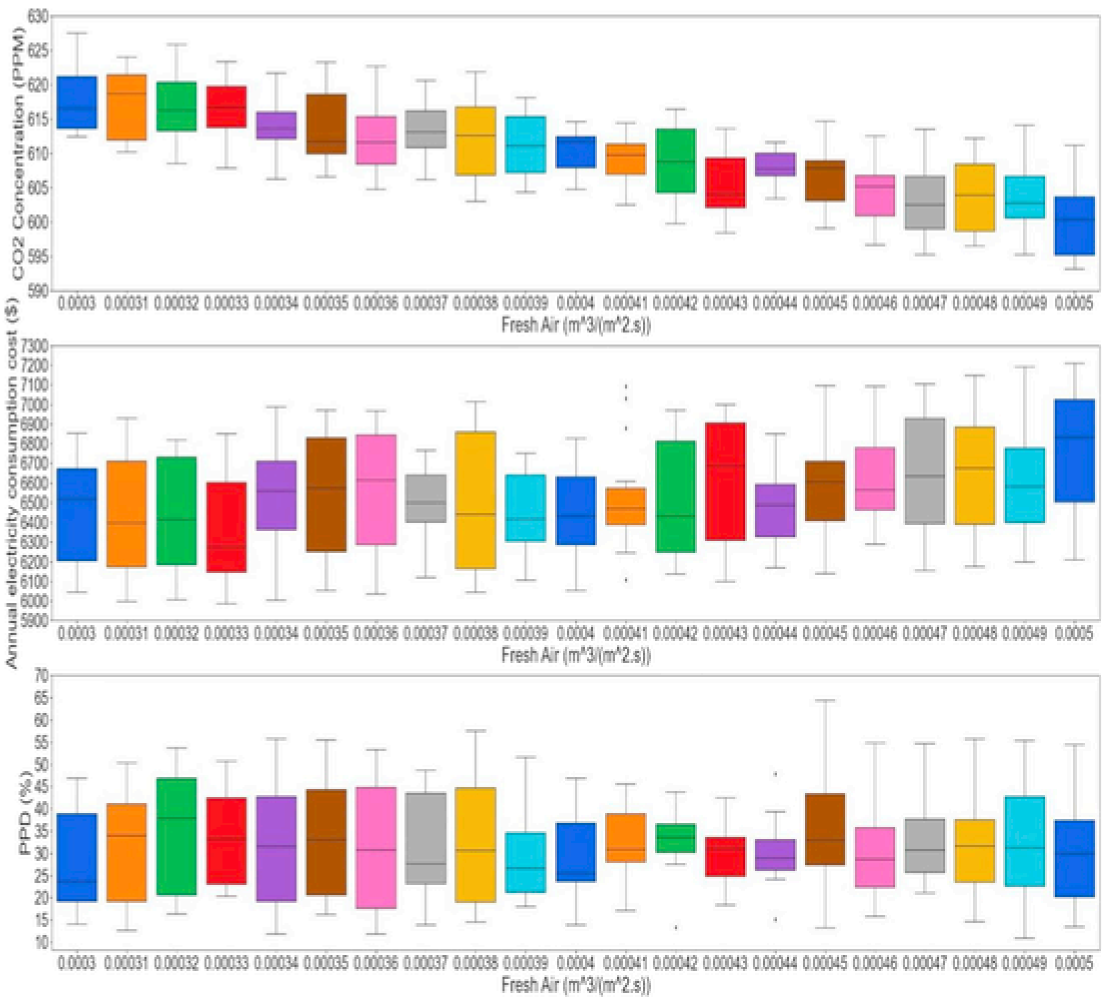

Fig. 15. The effect of fresh air on the objective functions for the city of Niwot Ridge.

Table 13
Optimal values of design variables and objective functions for six cities with different climates.

Cites	Heating set point (°C)	Cooling set point (°C)	Winter clothing insulation value (CLO)	Summer clothing insulation value (CLO)	Fresh Air $\left(\frac{m^3}{m^2.s}\right)$	CO_2 Concentration (PPM)	Annual electricity consumption cost ($)	PPD (%)
Cold Bay	21.2	25.7	1.2	0.7	0.00037	573.757	17957.67	19.83
Niwot Ridge	21.6	26.2	1.2	0.7	0.0003	613.41	6541.55	13.92
Key Biscayne	20.6	24.8	0.7	0.6	0.0005	600.5128	5238.28	7.811
Wendover	20.9	25	1.15	0.7	0.00039	607.13	5866.48	13.58
Midway	21.4	25.8	1.15	0.65	0.00038	615.11	5349.58	12.2
Rogers	19.9	25.7	1.1	0.55	0.00049	617.747	4767.55	15.72

Appendix.

ColdBay

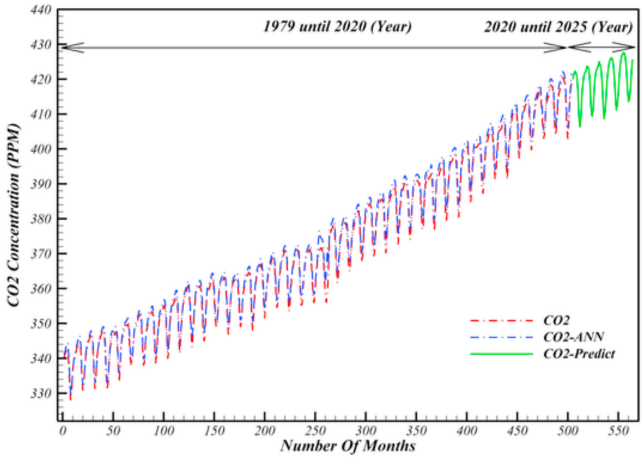

Objective	RMSE	R^2
CO_2	1.384	0.984442

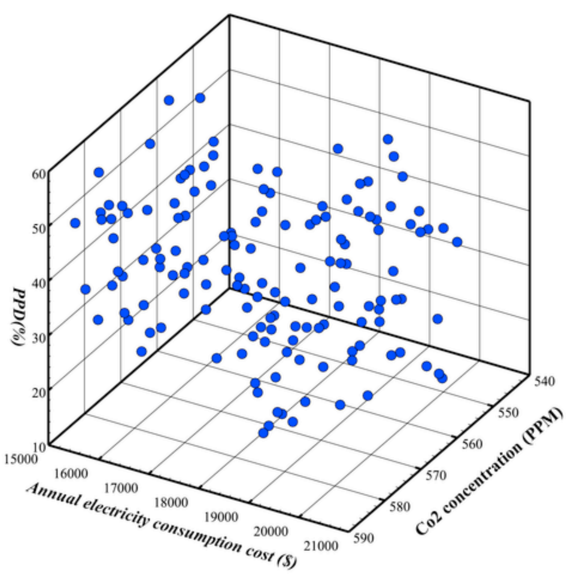

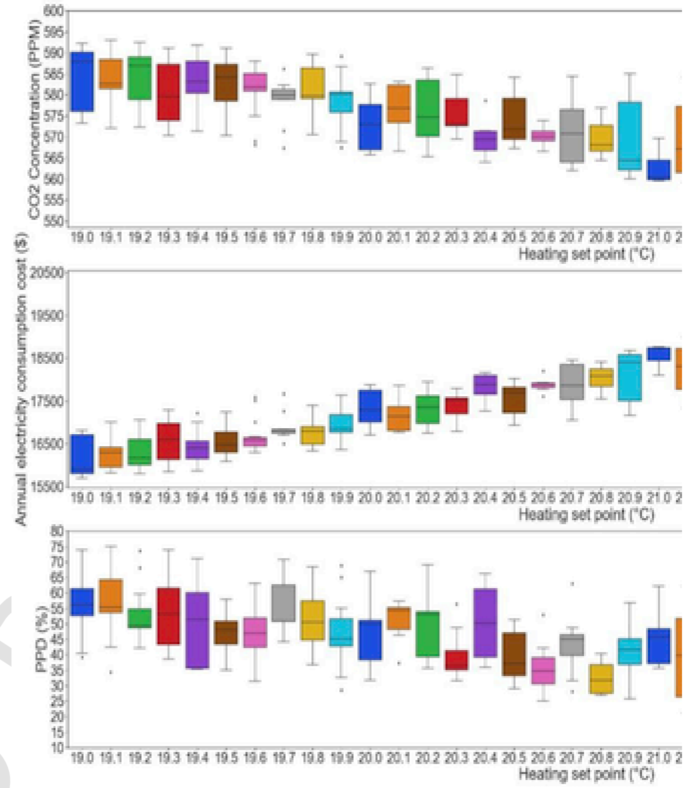

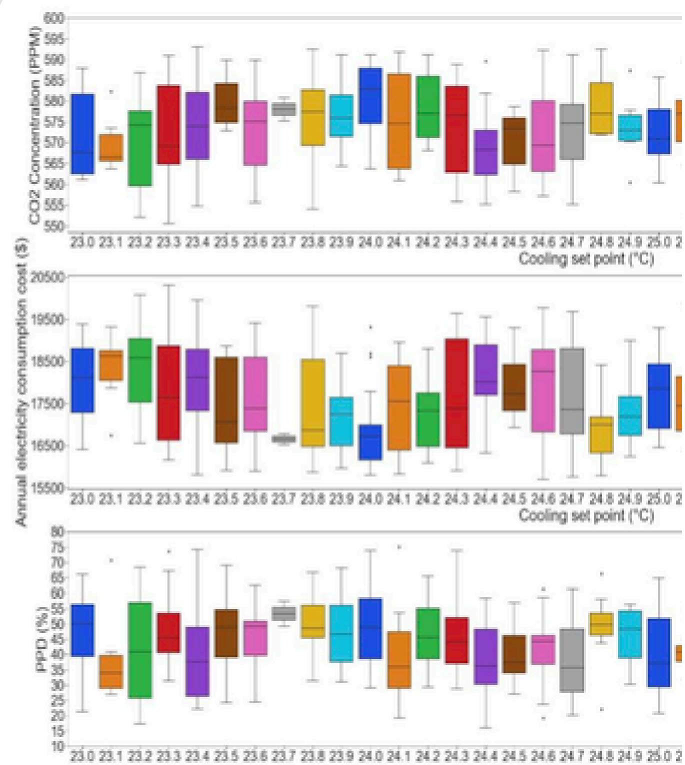

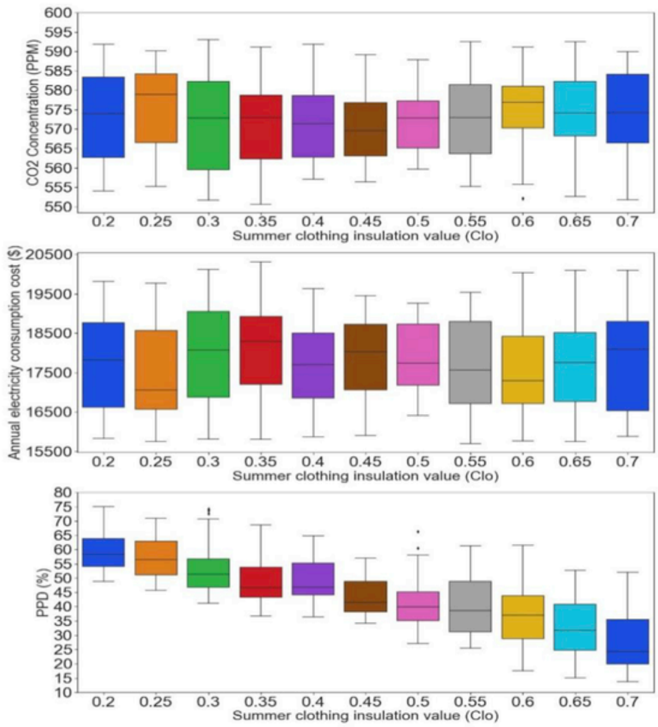

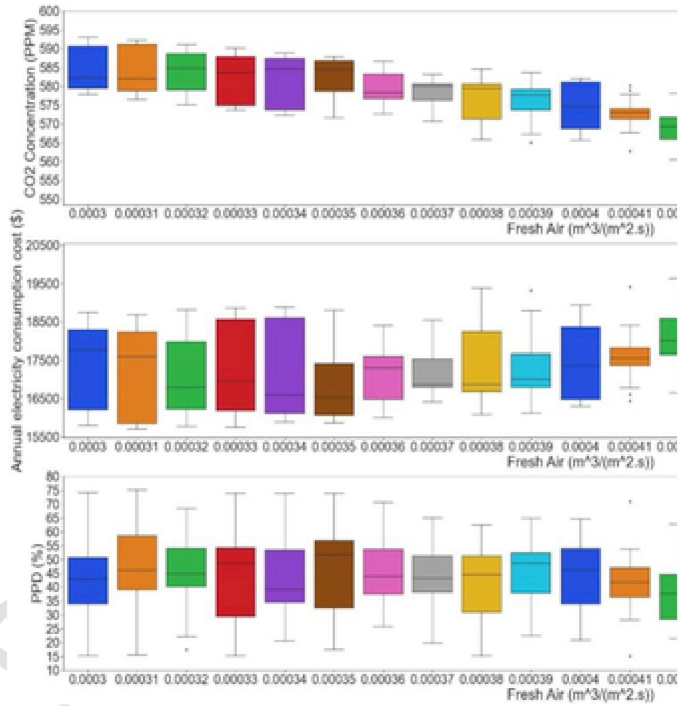

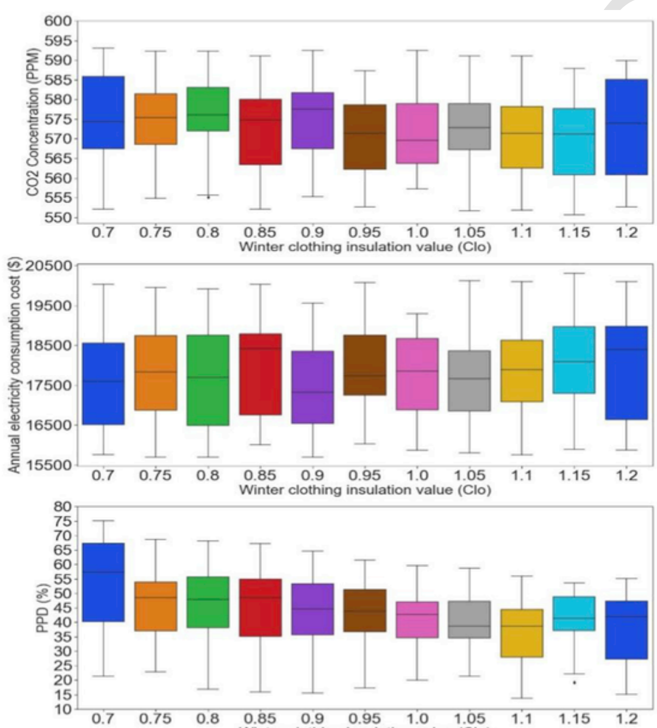

KeyBiscayne

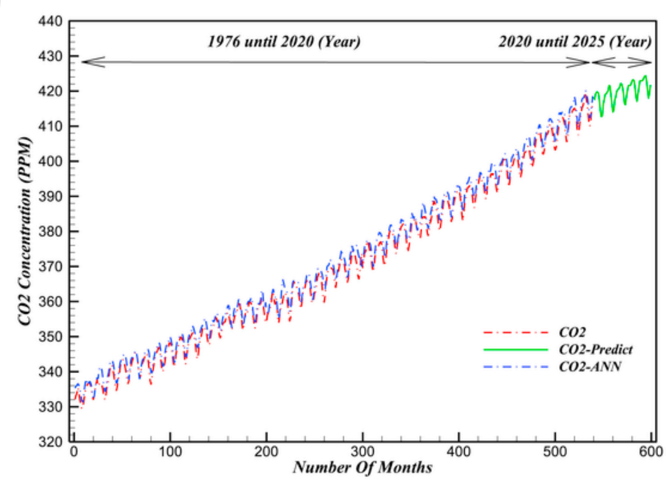

Objective	RMSE	R^2
CO_2	1.114	0.982075

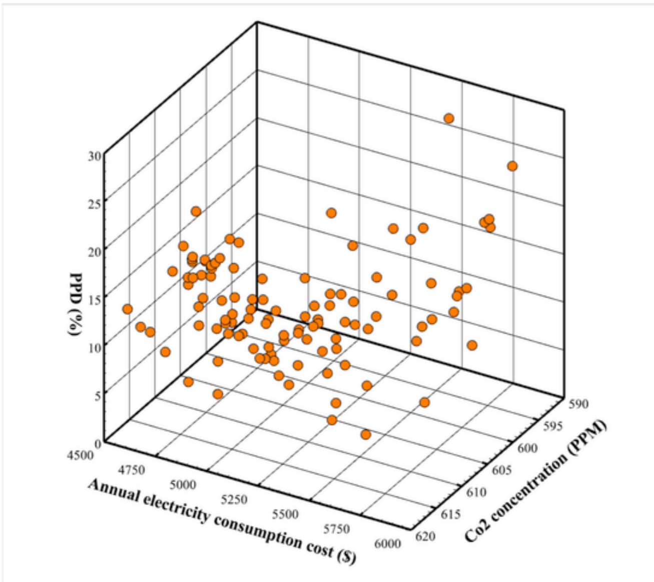
PPD (%)
Annual electricity consumption cost ($)
Co2 concentration (PPM)

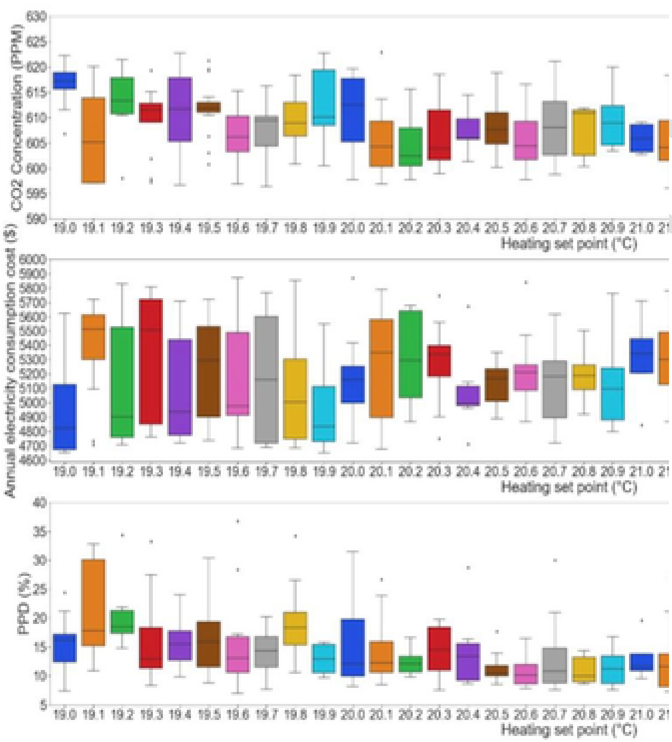
CO2 Concentration (PPM)
Annual electricity consumption cost ($)
PPD (%)
Heating set point (°C)

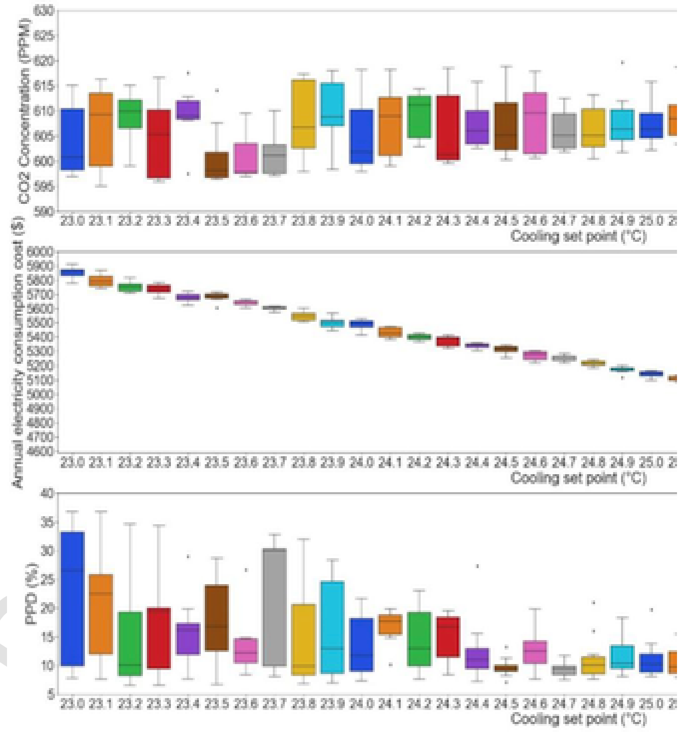
CO2 Concentration (PPM)
Annual electricity consumption cost ($)
PPD (%)
Cooling set point (°C)

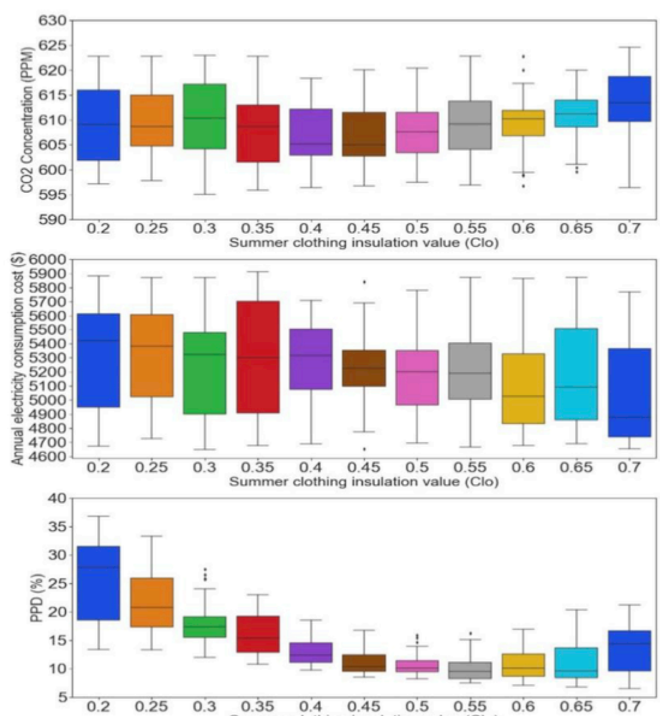
CO2 Concentration (PPM)
Annual electricity consumption cost ($)
PPD (%)
Summer clothing insulation value (Clo)

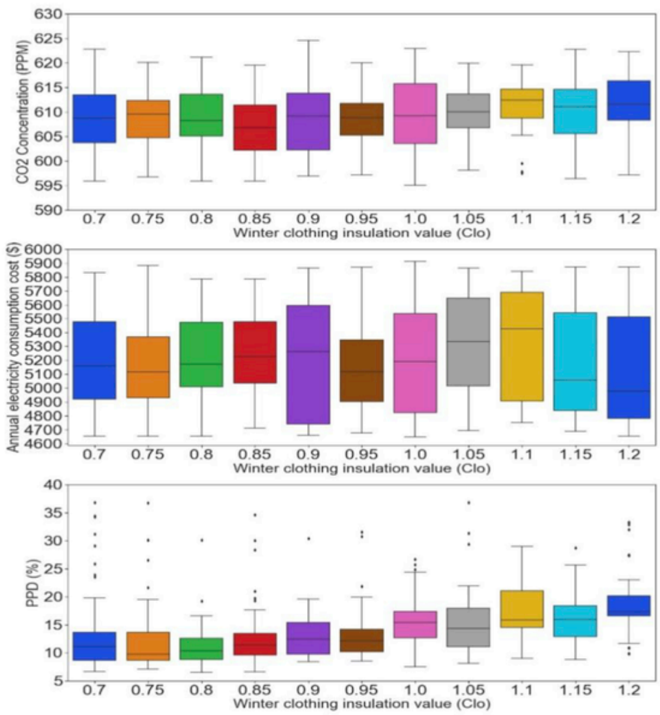

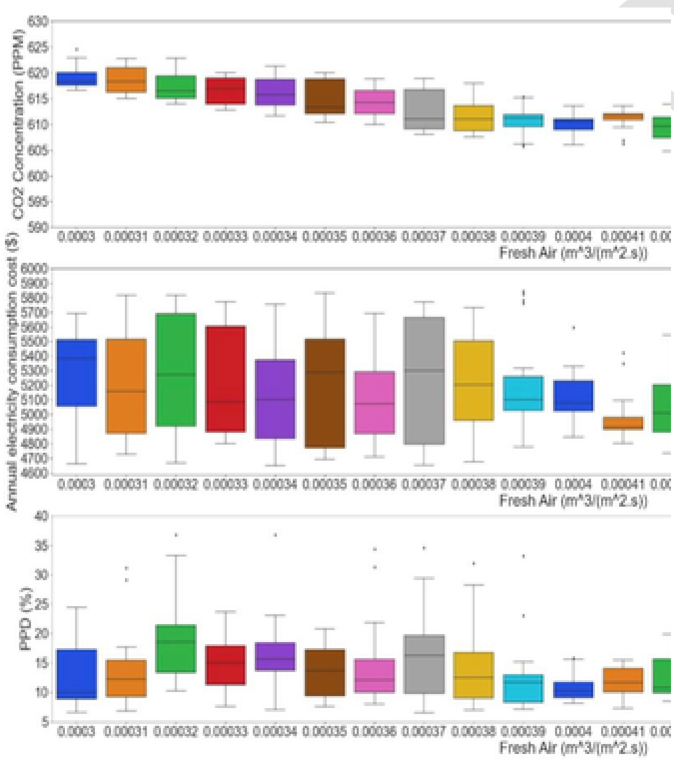

Wendover

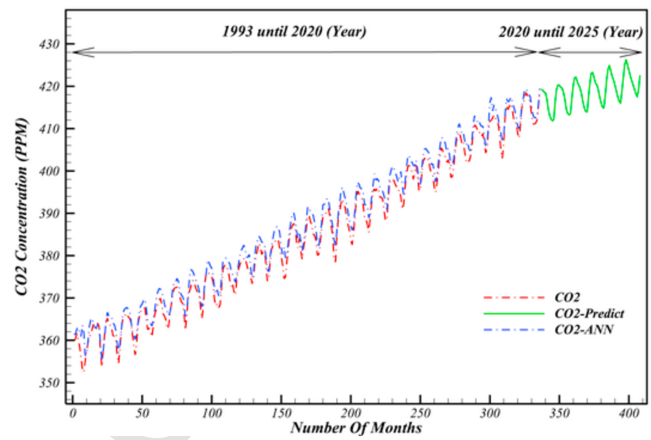

Objective	RMSE	R^2
CO2	1.083	0.985679

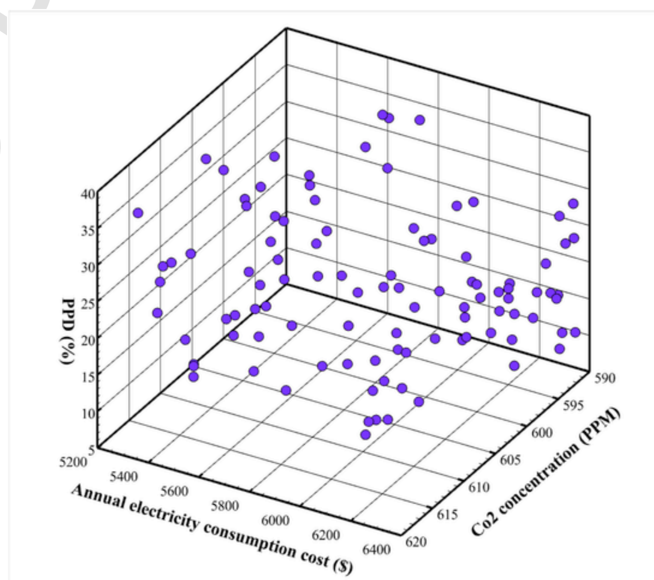

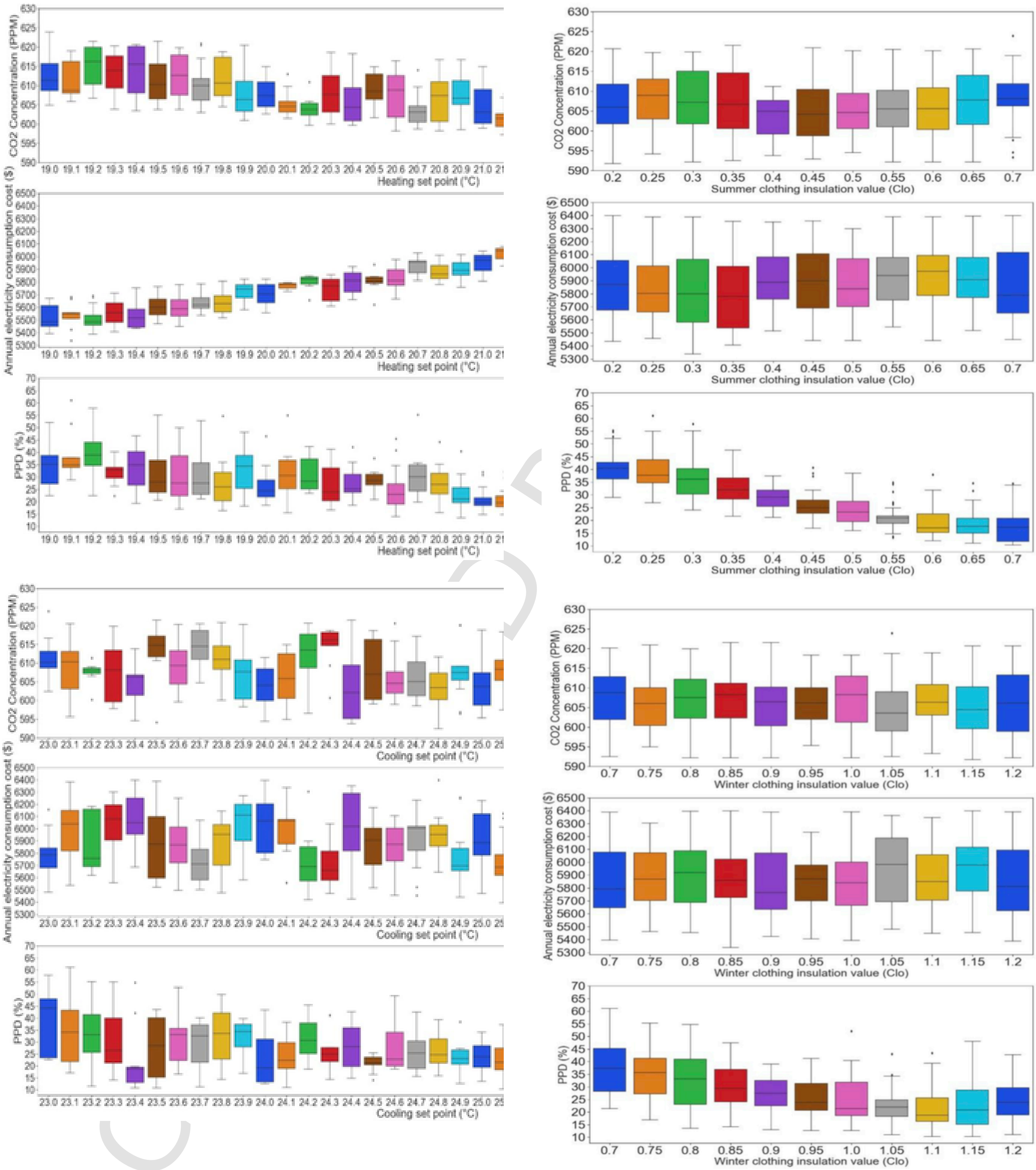
CO2 Concentration (PPM)
Heating set point (°C)
Annual electricity consumption cost ($)
PPD (%)
Cooling set point (°C)
Summer clothing insulation value (Clo)
Winter clothing insulation value (Clo)

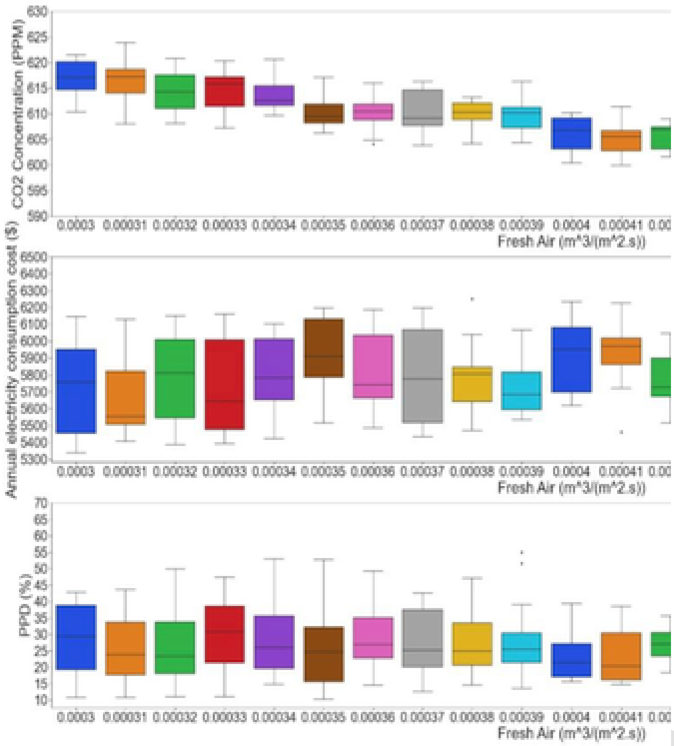

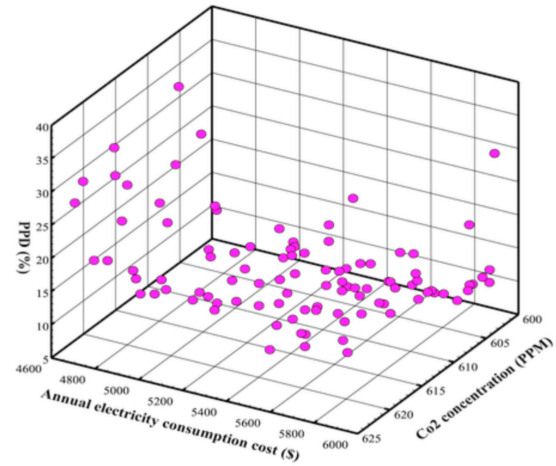

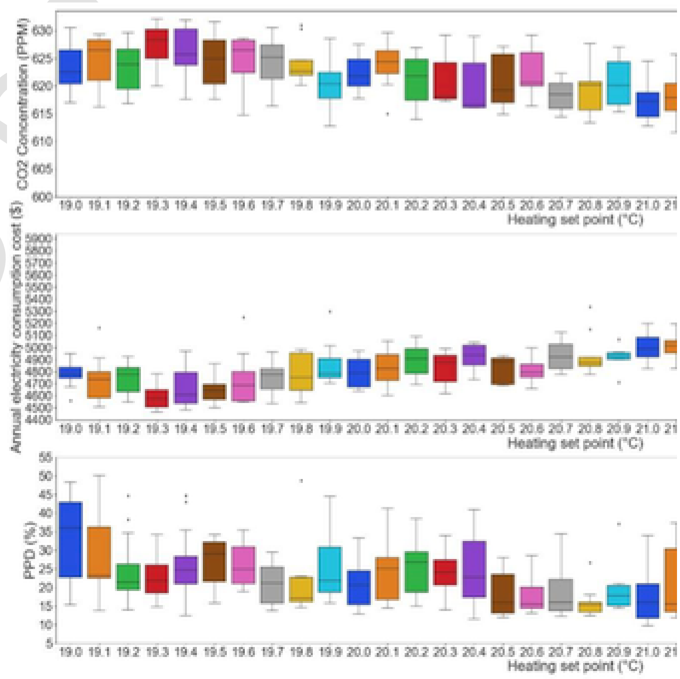

Midway

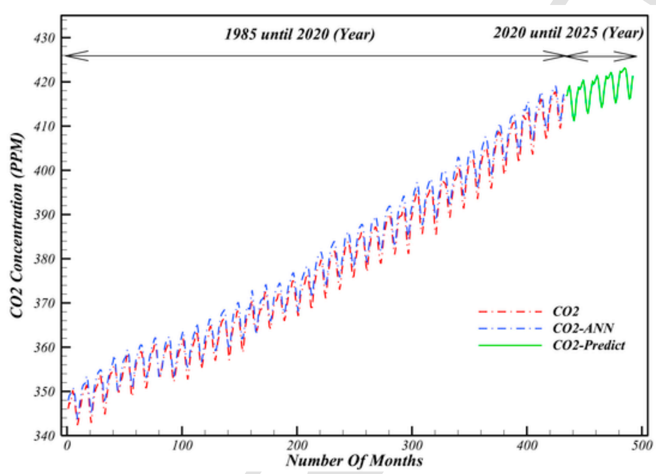

Objective	RMSE	R^2
CO2	0.6718	0.990086

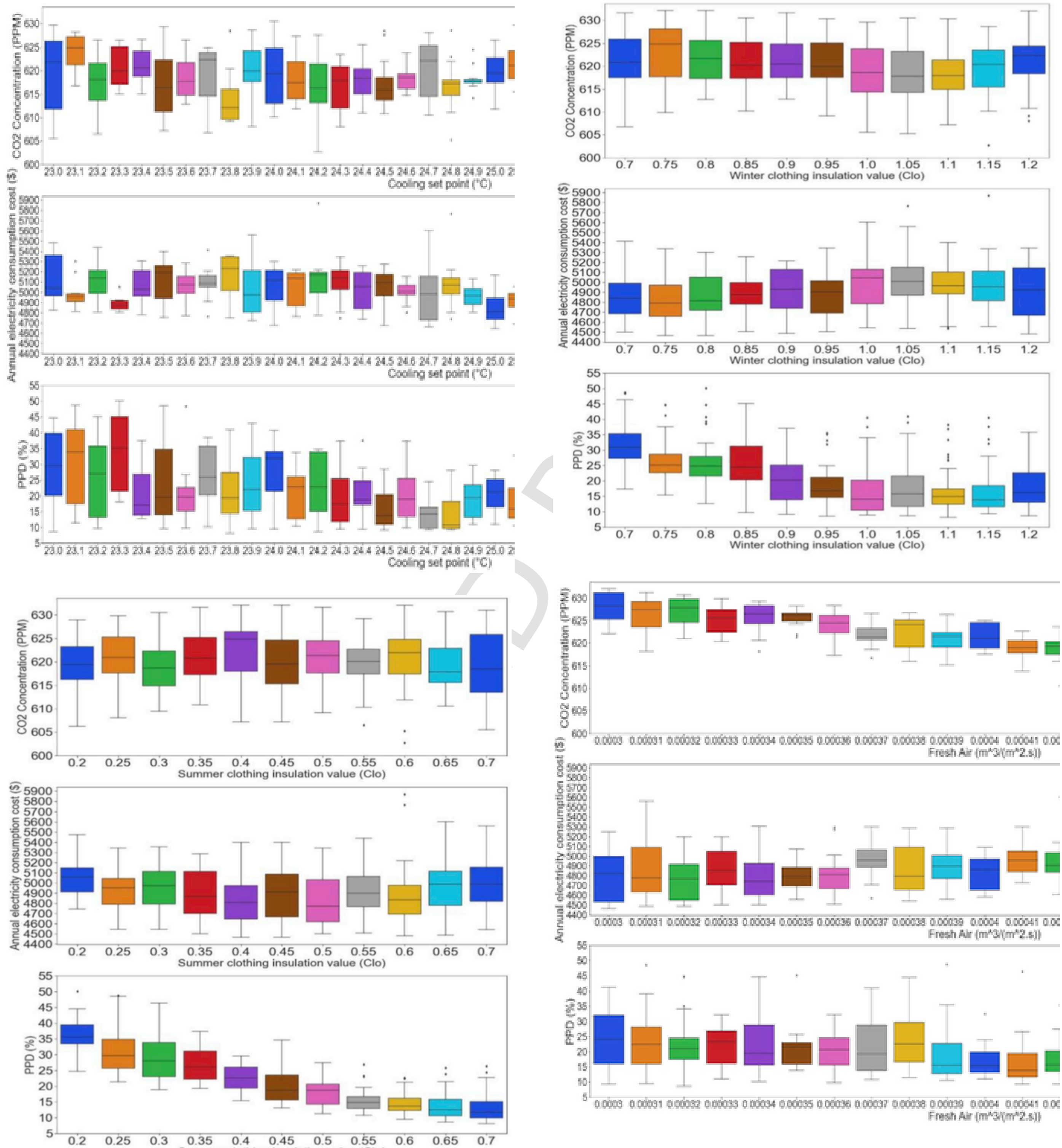
CO2 Concentration (PPM)
Cooling set point (°C)
Annual electricity consumption cost ($)
Cooling set point (°C)
PPD (%)
Cooling set point (°C)
CO2 Concentration (PPM)
Winter clothing insulation value (Clo)
Annual electricity consumption cost ($)
Winter clothing insulation value (Clo)
PPD (%)
Winter clothing insulation value (Clo)
CO2 Concentration (PPM)
Summer clothing insulation value (Clo)
Annual electricity consumption cost ($)
Summer clothing insulation value (Clo)
PPD (%)
Summer clothing insulation value (Clo)
CO2 Concentration (PPM)
Fresh Air (m^3/(m^2.s))
Annual electricity consumption cost ($)
Fresh Air (m^3/(m^2.s))
PPD (%)
Fresh Air (m^3/(m^2.s))

Rogers

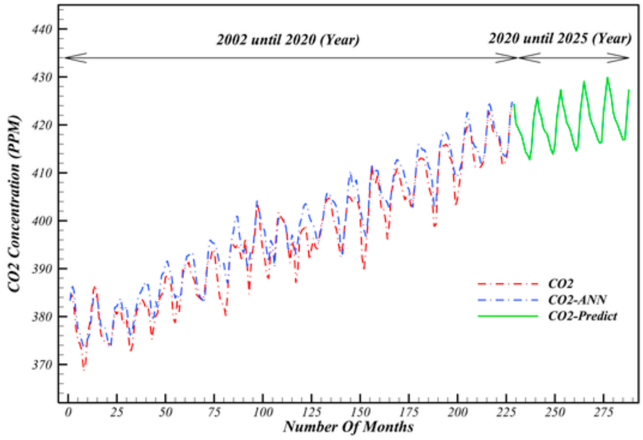

Objective	RMSE	R^2
CO2	1.27	0.985

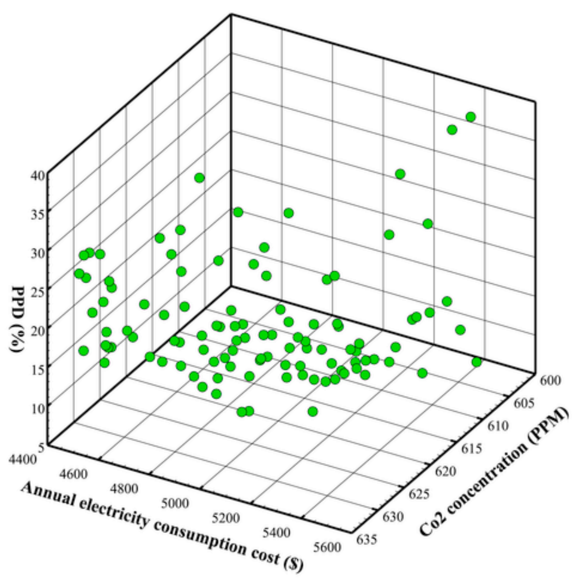

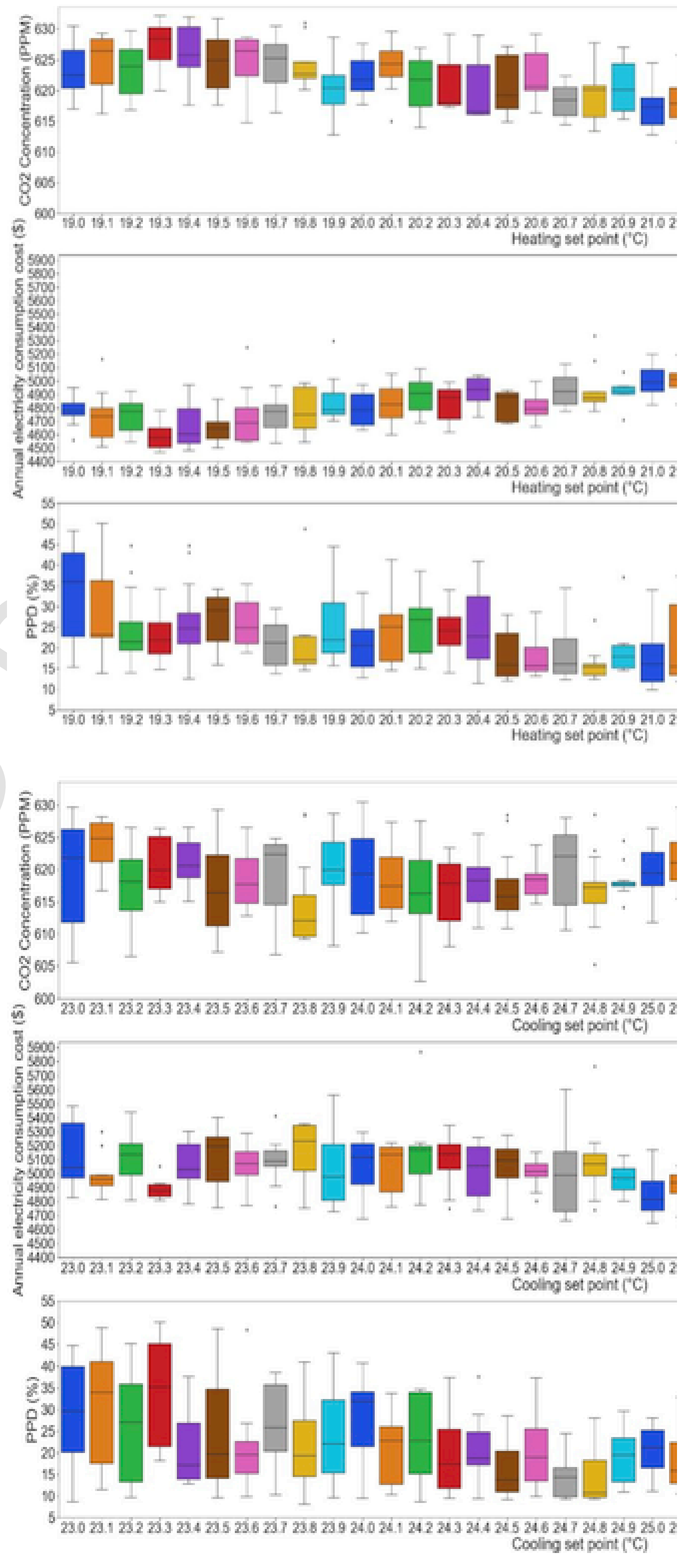

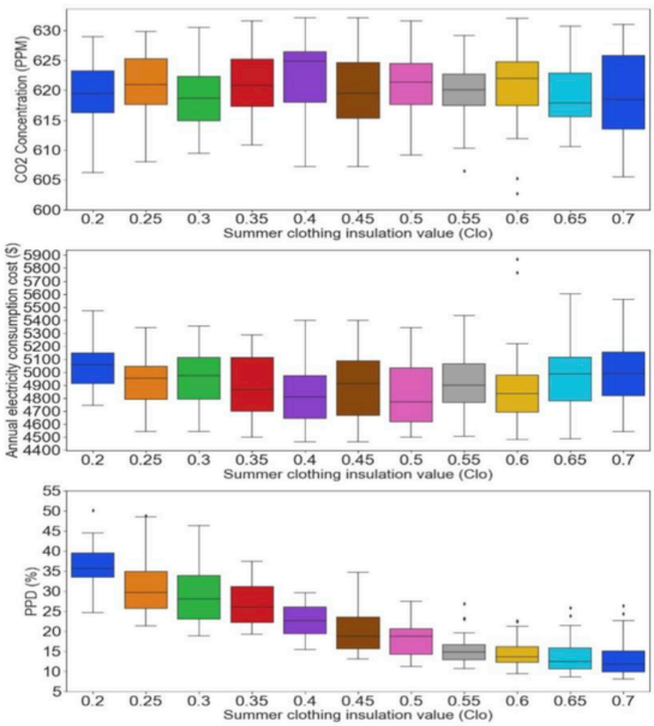

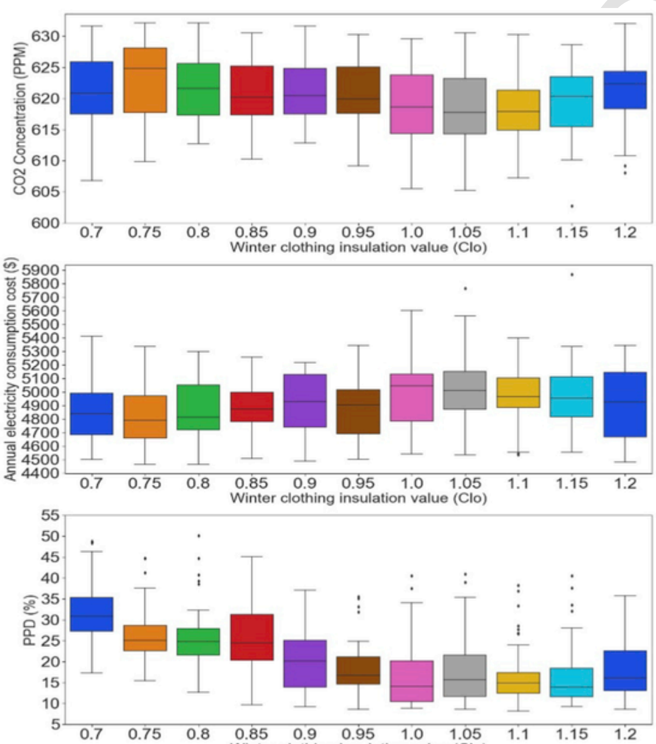

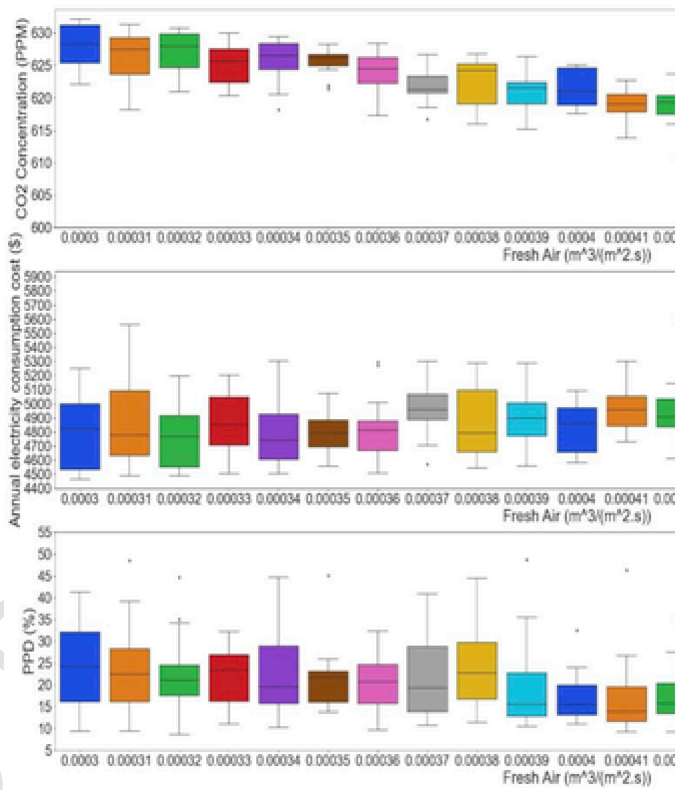

References

Abichou, T., et al., 2015. A novel approach to estimate methane oxidation in interim landfill covers across the USA. Int. J. Environ. Waste Manag. 15 (4), 309–326.

Agarkov, Nikolay B., Khaustov, Vladimir V., Malikov, Alexander M., Karpenko, Nikolay G., Ignatenko, Ignat M., 2022. Optimization of the drainage system of overburden dumps using geofiltration modeling. Caspian Journal of Environmental Sciences 20, no 1, 171–175.

Ahangari, M., Maerefat, M., 2019. An innovative PCM system for thermal comfort improvement and energy demand reduction in building under different climate conditions. Sustain. Cities Soc. 44, 120–129.

Ahmadi, G., Toghraie, D., Akbari, O., 2019. Energy, exergy and environmental (3E) analysis of the existing CHP system in a petrochemical plant. Renew. Sustain. Energy Rev. 99, 234–242.

Alghoul, S.K., 2017. A comparative study of energy consumption for residential hvac systems using EnergyPlus. American Journal of Mechanical and Industrial Engineering 2 (2), 98–103.

Amini, R., et al., 2021. Numerical investigation of indoor thermal comfort and air quality for a multi-purpose hall with various shading and glazing ratios. Therm. Sci. Eng. Prog. 22, 100812.

ANSI/ASHRAE, 2013. Standard 55, A., ASHRAE, Thermal environmental conditions for human occupancy. ANSI/ASHRAE Stand. 55, 2004.

Asadi, E., et al., 2012. A multi-objective optimization model for building retrofit strategies using TRNSYS simulations, GenOpt and MATLAB. Build. Environ. 56, 370–378.

ASHRAE 62.1, V.f.a.i.a.q, 2016. American Society of Heating. Refrigerating and Air-Conditioning Engineers, Atlanta.

Australian Building Codes Board (ABCB), I.A.Q.H, 2018. Australian Building Codes Board: Canberra. ACT.

Baghoolizadeh, M., et al., 2021. A multi-objective optimization of a building's total heating and cooling loads and total costs in various climatic situations using response surface methodology. Energy Rep. 7, 7520–7538.

Bahrami, A., Olsson, M., Svensson, K., 2022. Carbon dioxide emissions from various structural frame materials of single-family houses in nordic countries. International Journal of Innovative Research and Scientific Studies 5 (2), 112–120. https://doi.org/10.53894/ijirss.v5i2.414.

Bakos, G., 2000. Insulation protection studies for energy saving in residential and tertiary sector. Energy Build. 31 (3), 251–259.

Band, S.S., Al-Shourbaji, I., Karami, H., Karimi, S., Esfandiari, J., Mosavi, A., 2020a. Combination of group method of data handling (GMDH) and computational fluid dynamics (CFD) for prediction of velocity in channel intake. Appl. Sci. 10 (21), 7521.

Band, S.S., Mohammadzadeh, A., Csiba, P., Mosavi, A., Varkonyi-Koczy, A.R., 2020b. Voltage regulation for photovoltaics-battery-fuel systems using adaptive group method of data handling neural networks (GMDH-NN). IEEE Access 8, 213748–213757.

Batterman, S., et al., 2017. Ventilation rates in recently constructed US school classrooms. Indoor Air 27 (5), 880–890.

Bellos, E., et al., 2016. Energetic and financial evaluation of solar assisted heat pump space heating systems. Energy Convers. Manag. 120, 306–319.
Belmonte, J., Barbosa, R., Almeida, M.G., 2019. CO2 concentrations in a multifamily building in Porto, Portugal: occupants' exposure and differential performance of mechanical ventilation control strategies. J. Build. Eng. 23, 114–126.
Bojic, M., Yik, F., Sat, P., 2001. Influence of thermal insulation position in building envelope on the space cooling of high-rise residential buildings in Hong Kong. Energy Build. 33 (6), 569–581.
Bre, F., et al., 2016. Residential building design optimisation using sensitivity analysis and genetic algorithm. Energy Build. 133, 853–866.
Byčenkienė, S., Valuntaitė, V., Girgždienė, R., 2009. Simulation of indoor ozone concentration. Lith. J. Phys. 49 (3), 335–339. 335–339.
Canha, N., et al., 2017. Indoor air quality during sleep under different ventilation patterns. Atmos. Pollut. Res. 8 (6), 1132–1142.
Carlucci, S., et al., 2015. Multi-objective optimization of a nearly zero-energy building based on thermal and visual discomfort minimization using a non-dominated sorting genetic algorithm (NSGA-II). Energy Build. 104, 378–394.
Chen, R., Tsay, Y.-S., 2021. An integrated sensitivity analysis method for energy and comfort performance of an office building along the Chinese Coastline. Buildings 11 (8), 371.
Chen, T., Qi, C., Tang, J., Wang, G., Yan, Y., 2021. Numerical and experimental study on optimization of CPU system cooled by nanofluids. Case Stud. Therm. Eng. 24, 100848.
Chwieduk, D., 2003. Towards sustainable-energy buildings. Appl. Energy 76 (1–3), 211–217.
Coley, D.A., Greeves, R., Saxby, B.K., 2007. The effect of low ventilation rates on the cognitive function of a primary school class. Int. J. Vent. 6 (2), 107–112.
Dales, R., et al., 2008. Quality of indoor residential air and health. CMAJ (Can. Med. Assoc. J.) 179 (2), 147–152.
Daniels, R., Bodkin, A., 2016. Guidelines on ventilation, thermal comfort and indoor air quality in schools. Build. Bull. 101 (1), 1–109.
Deb, K., et al., 2002. A fast and elitist multiobjective genetic algorithm: NSGA-II. IEEE Trans. Evol. Comput. 6 (2), 182–197.
Delgarm, N., et al., 2016a. A novel approach for the simulation-based optimization of the buildings energy consumption using NSGA-II: case study in Iran. Energy Build. 127, 552–560.
Delgarm, N., Sajadi, B., Delgarm, S., 2016b. Multi-objective optimization of building energy performance and indoor thermal comfort: a new method using artificial bee colony (ABC). Energy Build. 131, 42–53.
Delgarm, N., et al., 2018. Sensitivity analysis of building energy performance: a simulation-based approach using OFAT and variance-based sensitivity analysis methods. J. Build. Eng. 15, 181–193.
Dianati Tilaki, G., Ahmadi Jolandan, M., Gholami, V., 2020. Rangelands production modeling using an artificial neural network (ANN) and geographic information system (GIS) in Baladeh rangelands, North Iran. Caspian J. Environ. Sci. 18 (3), 277–290.
Dorizas, P.V., Assimakopoulos, M.-N., Santamouris, M., 2015. A holistic approach for the assessment of the indoor environmental quality, student productivity, and energy consumption in primary schools. Environ. Monit. Assess. 187 (5), 1–18.
Fan, X., et al., 2021. Emission rate of carbon dioxide while sleeping. Indoor Air.
Farlow, S.J., 1984. Self-organizing Methods in Modeling GMDH Type Algorithms. Marcel Dekker, inc., New York.
Foroughi, R., Asadi, S., Khazaeli, S., 2021. On the optimization of energy efficient fenestration for small commercial buildings in the United States. J. Clean. Prod. 283, 124604.
Franco, A., Leccese, F., 2020. Measurement of CO2 concentration for occupancy estimation in educational buildings with energy efficiency purposes. J. Build. Eng. 32, 101714.
Gao, J., Wargocki, P., Wang, Y., 2014. Ventilation system type, classroom environmental quality and pupils' perceptions and symptoms. Build. Environ. 75, 46–57.
Guo, R., et al., 2019. Influence of design parameters on the night ventilation performance in office buildings based on sensitivity analysis. Sustain. Cities Soc. 50, 101661.
Haddad, S., et al., 2021. On the potential of demand-contsrolled ventilation system to enhance indoor air quality and thermal condition in Australian school classrooms. Energy Build. 238, 110838.
Heebøll, A., Wargocki, P., Toftum, J., 2018. Window and door opening behavior, carbon dioxide concentration, temperature, and energy use during the heating season in classrooms with different ventilation retrofits—ASHRAE RP1624. Sci. Technol. Built Environ. 24 (6), 626–637.
Henninger, R.H., Witte, M.J., Crawley, D.B., 2004. Analytical and comparative testing of EnergyPlus using IEA HVAC BESTEST E100–E200 test suite. Energy Build. 36 (8), 855–863.
https://gml.noaa.gov/.
Huo, H., et al., 2021. Analysis and optimization of external Venetian blind shading for nearly zero-energy buildings in different climate regions of China. Sol. Energy 223, 54–71.
IPCC, 2014. Intergovernmental panel on climate change. Climate change 2014:mitigation of climate change. Chapter 9: Buildings.
Ivakhnenko, A.G., 1971. Polynomial theory of complex systems. IEEE Transact. Syst. Man Cybernetics (4), 364–378.
Jaber, A.R., Dejan, M., Marcella, U., 2017. The effect of indoor temperature and CO2 levels on cognitive performance of adult females in a university building in Saudi Arabia. Energy Proc. 122, 451–456.
Jermsittiparsert, K., 2021. Examining the sustainable energy and carbon emission on the economy: panel evidence from asean. Int. J. Econ. Finance Stud. 13 (1), 405–426.
Jia, Qi, Wang, Tiening, 2021. Research on supply optimization decision of over storage equipment. J. Ordnance Equipment Eng. 42, 131–136. 02.
Jung, C., Awad, J., 2021. Improving the IAQ for learning efficiency with indoor plants in university classrooms in Ajman, United Arab Emirates. Buildings 11 (7), 289.
Kamal, R., et al., 2019. Strategic control and cost optimization of thermal energy storage in buildings using EnergyPlus. Appl. Energy 246, 77–90.
Karmellos, M., Kiprakis, A., Mavrotas, G., 2015. A multi-objective approach for optimal prioritization of energy efficiency measures in buildings: model, software and case studies. Appl. Energy 139, 131–150.
Khoukhi, M., 2018. The combined effect of heat and moisture transfer dependent thermal conductivity of polystyrene insulation material: impact on building energy performance. Energy Build. 169, 228–235.
Korsavi, S.S., Montazami, A., Mumovic, D., 2020. Ventilation rates in naturally ventilated primary schools in the UK; Contextual, Occupant and Building-related (COB) factors. Build. Environ. 181, 107061.
Kumar, R., Nagar, J., Gaur, S., 2005. Indoor air pollutants and respiratory morbidity-a review. Indian Journal of Allergy. Asthma and Immunology 19 (1), 1–9.
Leech, J.A., et al., 2002. It's about time: a comparison of Canadian and American time–activity patterns. J. Expo. Sci. Environ. Epidemiol. 12 (6), 427–432.
Li, Cuicui, Yi, Wenjun, Guan, Jun, et al., 2021. Fuzzy PID control of electromechanical Actuator system based on genetic algorithm. J. Ordnance Equipment Eng. 42, 162–167. 03.
Lin, L., Chen, C., Wei, B., et al., 2022. Residential electricity load scenario prediction based on transferable flow generation model. J. Electr. Eng. Technol. https://doi.org/10.1007/s42835-022-01172-6.
Liu, C., Qiao, Y., Du, P., Zhang, J., Zhao, J., Liu, C., Huo, Y., Qi, C., Rao, Z., Yan, Y., 2021. Recent advances of nanofluids in micro/nano scale energy transportation. Renew. Sustain. Energy Rev. 149, 111346.
Loni, R., et al., 2018. GMDH modeling and experimental investigation of thermal performance enhancement of hemispherical cavity receiver using MWCNT/oil nanofluid. Sol. Energy 171, 790–803.
Lu, Shanshan, Wang, Zhisheng, Ouyang, Quan, et al., 2021. Simulation of compound control based on fuzzy PI and artificial neural network for Aircraft electromechanical Actuation systems. J. Ordnance Equipment Eng. 42 (10), 158–164.
Madandoust, R., Ghavidel, R., Nariman-Zadeh, N., 2010. Evolutionary design of generalized GMDH-type neural network for prediction of concrete compressive strength using UPV. Comput. Mater. Sci. 49 (3), 556–567.
Mashrae, Y.Z.P., Use jEPlus as an Efficient Building Design Optimisation Tool.
Mateus, N.M., Pinto, A., Da Graça, G.C., 2014. Validation of EnergyPlus thermal simulation of a double skin naturally and mechanically ventilated test cell. Energy Build. 75, 511–522.
McGill, G., Oyedele, L.O., McAllister, K., 2015. Case study investigation of indoor air quality in mechanically ventilated and naturally ventilated UK social housing. Int. J. Sustain. Built Environ. 4 (1), 58–77.
Morris, M.D., 1991. Factorial sampling plans for preliminary computational experiments. Technometrics 33 (2), 161–174.
Muruganantham, K., 2010. Application of Phase Change Material in Buildings: Field Data vs. EnergyPlus Simulation. Arizona State University.
Nabipour, N., Dehghani, M., Mosavi, A., Shamshirband, S., 2020. Short-term hydrological drought forecasting based on different nature-inspired optimization algorithms hybridized with artificial neural networks. IEEE Access 8, 15210–15222.
Naboni, E., et al., 2013. Extending the use of parametric simulation in practice through a cloud based online service. In: IBPSA Italy-Conference of International Building Performance Simulation Association. Bozen, Italy.
Naderi, E., et al., 2020. Multi-objective simulation-based optimization of controlled blind specifications to reduce energy consumption, and thermal and visual discomfort: case studies in Iran. Build. Environ. 169, 106570.
Naji, S., Aye, L., Noguchi, M., 2021. Sensitivity analysis on energy performance, thermal and visual discomfort of a prefabricated house in six climate zones in Australia. Appl. Energy 298, 117200.
Noris, F., et al., 2013. Indoor environmental quality benefits of apartment energy retrofits. Build. Environ. 68, 170–178.
Pandey, B., Banerjee, R., Sharma, A., 2021. Coupled EnergyPlus and CFD analysis of PCM for thermal management of buildings. Energy Build. 231, 110598.
Parhizkar, H., Khoraskani, R.A., Tahbaz, M., 2020. Double skin façade with Azolla; ventilation, indoor air quality and thermal performance assessment. J. Clean. Prod. 249, 119313.
Pereira, W., Bögl, A., Natschläger, T., 2014. Sensitivity analysis and validation of an EnergyPlus model of a house in Upper Austria. Energy Proc. 62, 472–481.
Pereira, P.F., et al., 2017. Occupant influence on residential ventilation patterns in mild climate conditions. Energy Proc. 132, 837–842.
Qi, C., Li, C., Li, K., Han, D., 2022. Natural convection of nanofluids in solar energy collectors based on a two-phase lattice Boltzmann model. J. Therm. Anal. Calorim. 147 (3), 2417–2438.
Refat, K.H., Sajjad, R.N., 2020. Prospect of achieving net-zero energy building with semi-transparent photovoltaics: a device to system level perspective. Appl. Energy 279, 115790.
Rosso, F., et al., 2020. Multi-objective optimization of building retrofit in the Mediterranean climate by means of genetic algorithm application. Energy Build. 216, 109945.
Rostamzadeh-Renani, M., et al., 2022. The Effect of Canard's Optimum Geometric Design on Wake Control behind the Car Using Artificial Neural Network and Genetic Algorithm. ISA Transactions.
Rustamovich Sultanbekov, I., Yurievna Myshkina, I., Yurievna Gruditsyna, L., 2020. Development of an application for creation and learning of neural networks to utilize in environmental sciences. Caspian J. Environ. Sci. 18 (5), 595–601.
Ryu, J.-h., Kim, S., Wan, H., 2009. Pareto front approximation with adaptive weighted sum method in multiobjective simulation optimization. In: Proceedings of the 2009

Winter Simulation Conference (WSC). IEEE.
Said, Zafar, Sundar, L. Syam, Rezk, Hegazy, Nassef, Ahmed M., Chakraborty, Samarshi, Li, Changhe, 2021. Thermophysical properties using ND/water nanofluids: an experimental study, ANFIS-based model and optimization. J. Mol. Liq. 330, 115659. https://doi.org/10.1016/j.molliq.2021.115659.
Said, Z., Ghodbane, M., Boumeddane, B., Tiwari, A.K., Sundar, S., Li, C.H., Aslfattahi, N., Bellos, E., 2022. Energy, exergy, economic and environmental (4E) analysis of a parabolic trough solar collector using MXene based silicone oil nanofluids. Sol. Energy Mater. Sol. Cell. 239, 111633. https://doi.org/10.1016/j.solmat.2022.111633.
Sanchez, E., Shibata, T., Zadeh, L.A., 1997. Genetic Algorithms and Fuzzy Logic Systems: Soft Computing Perspectives, vol. 7. World Scientific.
Santamouris, M., et al., 2008. Experimental investigation of the air flow and indoor carbon dioxide concentration in classrooms with intermittent natural ventilation. Energy Build. 40 (10), 1833–1843.
Schibuola, L., Scarpa, M., Tambani, C., 2016. Natural ventilation level assessment in a school building by CO2 concentration measures. Energy Proc. 101, 257–264.
Shabri, A., Samsudin, R., 2014. A hybrid GMDH and box-jenkins models in time series forecasting. Appl. Math. Sci. 8 (62), 3051–3062.
Shahsavar, A., et al., 2019. A novel comprehensive experimental study concerned synthesizes and prepare liquid paraffin-Fe3O4 mixture to develop models for both thermal conductivity & viscosity: a new approach of GMDH type of neural network. Int. J. Heat Mass Tran. 131, 432–441.
Shang, K., Chen, Z., Liu, Z., Song, L., Zheng, W., Yang, B., et al., 2021. Haze prediction model using deep recurrent neural network. Atmosphere 12 (12), 1625. https://doi.org/10.3390/atmos12121625.
Solgi, E., Memarian, S., Moud, G.N., 2018. Financial viability of PCMs in countries with low energy cost: a case study of different climates in Iran. Energy Build. 173, 128–137.
Srinivasan, D., 2008. Energy demand prediction using GMDH networks. Neurocomputing 72 (1–3), 625–629.
Srinivasareddy, R.S., Narayana, Y.V., Krishna, D., 2021. Sector beam synthesis in linear Antenna Arrays using social group optimization algorithm. Nat. J. Antennas Propagation 3 (2), 6–9. https://doi.org/10.31838/NJAP/03.02.02.
Sundell, J., 2004. On the history of indoor air quality and health. Indoor Air 14 (s 7), 51–58.
Synnefa, A., Santamouris, M., Akbari, H., 2007. Estimating the effect of using cool coatings on energy loads and thermal comfort in residential buildings in various climatic conditions. Energy Build. 39 (11), 1167–1174.
Tabares-Velasco, P.C., et al., 2012. Verification and Validation of EnergyPlus Conduction Finite Difference and Phase Change Material Models for Opaque Wall Assemblies. National Renewable Energy Lab.(NREL), Golden, CO (United States).
Tu, J., Qi, C., Zhang, S., Tang, Z., 2022. Comprehensive thermal-hydraulic performance and thermoelectric conversion efficiency of bionic battery waste heat recovery system. J. Energy Storage 48, 104039.
U. EIA, "Energy Information Administration" International Energy Outlook, report DOE/EIA-04842016.
US Department of Energy, 2014. Office of energy efficiency & renewable energy. EnergyPlus Doc.
Wang, H., Hou, K., Zhao, J., Yu, X., Jia, H., et al., 2022. Planning-Oriented resilience assessment and enhancement of integrated electricity-gas system considering multi-type natural disasters. Appl. Energy 315. https://doi.org/10.1016/j.apenergy.2022.118824.
Wiryadinata, S., et al., 2016. Technical and economic feasibility of unitary, horizontal ground-loop geothermal heat pumps for space conditioning in selected California climate zones. Energy Build. 119, 164–172.
www.eia.gov.
Xie, X., Sun, Y., 2022. A piecewise probabilistic harmonic power flow approach in unbalanced residential distribution systems. Int. J. Electr. Power Energy Syst. 141, 108114. https://doi.org/10.1016/j.ijepes.2022.108114.
Yan, S.R., et al., 2020. Energy efficiency optimization of the waste heat recovery system with embedded phase change materials in greenhouses: a thermo-economic-environmental stud. J. Energy Storage 30, 101445.
Yang, M.-D., et al., 2016. Multiobjective optimization using nondominated sorting genetic algorithm-II for allocation of energy conservation and renewable energy facilities in a campus. Energy Build. 122, 120–130.
Zhai, Y., et al., 2019. A multi-objective optimization methodology for window design considering energy consumption, thermal environment and visual performance. Renew. Energy 134, 1190–1199.
Zhang, Y., 2012. Use jEPlus as an efficient building design optimisation tool. In: CIBSE ASHRAE Technical Symposium. Imperial College London.
Zhang, Y., Korolija, I., 2010. Performing complex parametric simulations with jEPlus. In: SET2010-9th International Conference on Sustainable Energy Technologies.
Zhang, Z., Tian, J., Huang, W., Yin, L., Zheng, W., et al., 2021. A haze prediction method based on one-dimensional Convolutional neural network. Atmosphere 12 (10), 1327. https://doi.org/10.3390/atmos12101327.
Zhang, Y., Shi, X., Zhang, H., Cao, Y., Terzija, V., 2022. Review on deep learning applications in frequency analysis and control of modern power system. Int. J. Electr. Power Energy Syst. 136, 107744. https://doi.org/10.1016/j.ijepes.2021.107744.
Zor, K., et al., 2020. Short-term building electrical energy consumption forecasting by employing gene expression programming and GMDH networks. Energies 13 (5), 1102.